

## **Copyright Warning & Restrictions**

The copyright law of the United States (Title 17, United States Code) governs the making of photocopies or other reproductions of copyrighted material.

Under certain conditions specified in the law, libraries and archives are authorized to furnish a photocopy or other reproduction. One of these specified conditions is that the photocopy or reproduction is not to be “used for any purpose other than private study, scholarship, or research.” If a user makes a request for, or later uses, a photocopy or reproduction for purposes in excess of “fair use” that user may be liable for copyright infringement,

This institution reserves the right to refuse to accept a copying order if, in its judgment, fulfillment of the order would involve violation of copyright law.

**Please Note: The author retains the copyright while the New Jersey Institute of Technology reserves the right to distribute this thesis or dissertation**

Printing note: If you do not wish to print this page, then select “Pages from: first page # to: last page #” on the print dialog screen

The Van Houten library has removed some of the personal information and all signatures from the approval page and biographical sketches of theses and dissertations in order to protect the identity of NJIT graduates and faculty.

## **ABSTRACT**

### **DECONTAMINATION OF AQUIFERS VIA AIR SPARGING/BIOFILTRATION: AN EXPERIMENTAL STUDY**

**by**  
**Armando Mora Tellez**

In this study experiments were performed in order to show feasibility of an integrated air sparging/biofiltration process for cleaning contaminated groundwater. Feasibility was also meant in the sense of meeting regulatory constraints. Using toluene as model compound and changing flowrates for the sparged air, it was shown that despite fluctuations in the toluene concentration at the inlet of the biofilter, the concentrations at the outlet of the unit were essentially constant over long periods of time and remained below the levels dictated by environmental regulations. However an increase in outlet concentrations at levels not meeting regulatory constraints was observed after the first phases of the process. This failure is attributed to poor moisture control in the biofilter bed.

Experiments with the air sparging process alone, aiming at describing the distribution of the pollutant between contaminated water and air sparged through it showed that this distribution is a function of the pollutant concentration in the water and the residence time of the sparged air in the water reservoir. However, efforts to model and mathematically describe this distribution have failed and led to no significant conclusions.

**DECONTAMINATION OF AQUIFERS VIA AIR SPARGING/BIOFILTRATION:  
AN EXPERIMENTAL STUDY**

by  
**Armando Mora Tellez**

**A Thesis  
Submitted to the Faculty of  
New Jersey Institute of Technology  
in Partial Fulfillment of the Requirements for the Degree of  
Master of Science in Chemical Engineering**

**Department of Chemical Engineering,  
Chemistry, and Environmental Science**

**May 1997**

Blank Page

APPROVAL PAGE

DECONTAMINATION OF AQUIFERS VIA AIR SPARGING/BIOFILTRATION:  
AN EXPERIMENTAL STUDY

Armando Mora Tellez

---

Dr. Basil C. Baltzis, Dissertation Advisor Date  
Professor of Chemical Engineering, NJIT

---

Dr. Piero M. Armenante, Committee Member Date  
Professor of Chemical Engineering, NJIT

---

Dr. Dana E. Knox, Committee Member Date  
Associate Professor of Chemical Engineering, NJIT

## BIOGRAPHICAL SKETCH

**Author:** Armando Mora Tellez

**Degree:** Master of Science

**Date:** May 1997

### **Undergraduate and Graduate Education:**

- Master of Science in Chemical Engineering (Fulbright),  
New Jersey Institute of Technology, Newark, NJ, 1997
- Certificate,  
Continuous Education Program at Metropolitan Autonomous University,  
Mexico City, "Environmental Risk Assessment", 1993
- Bachelor of Science in Chemical Engineering,  
Metropolitan Autonomous University, Mexico City, 1993

**Major:** Chemical Engineering

This thesis is dedicated to  
my parents Ildefonso and Etelvina Mora  
and  
to the loving memory of my grandparents Linda and Andres



## ACKNOWLEDGMENT

The author would like to express his sincere gratitude to his thesis advisor, Dr. Basil C. Baltzis, for his expert guidance throughout this research. The author is grateful to Professors Piero M. Armenante and Dana E. Knox for serving as members of the committee.

The author appreciates the help, support and friendship of his fellow students including: Dr. Socratis Ioannidis, Dilip Mandal and Christos Mpanias.

The author would like to sincerely express his appreciation to Donato de la Cruz and Gwen San Agustin for their unconditional support and life encouragement.

The author appreciates the help, support and friendship of his friends: Sergio Mora, Fernando Camacho, Olimpia Cervantes, Leopoldo Mira, Hendrik Roscher, Alex Rothaker, Etienne Butruille, Johan Resare, Doris Yacoub and Daniela Vanata. Special thanks to his friends Martin Peter for his support and Rajive Shah for his unconditional help.

The author would also like to express thanks to Mario and Tina Mora for their advice and support.

Finally, the author would also like to sincerely express his appreciation and love to his family for their constant support: Ildefonso, Octavio, Nayeli and Lucero Mora.

## TABLE OF CONTENTS

Chapter	Page
1 INTRODUCTION.....	1
2 LITERATURE REVIEW.....	4
2.1 Multiphase Contamination.....	4
2.2 Air Sparging.....	5
2.3 Biofiltration.....	8
3 OBJECTIVES.....	14
4 DESCRIPTION OF POLLUTANT DISTRIBUTION BETWEEN WATER AND SPARGED AIR.....	19
5 EXPERIMENTAL APPROACH AND PROCEDURES.....	22
5.1 Apparatus for the Air Sparging/Biofiltration Studies.....	22
5.2 Apparatus for the Toluene Distribution Experiments.....	24
5.3 Materials.....	25
5.4 Analytical.....	25
5.5 Procedures for the Air Sparging/Biofiltration Experiments.....	26
5.6 Procedures for the Toluene Distribution Experiments.....	28
6 RESULTS AND DISCUSSION.....	29
6.1 Preliminary Biofilter Experiments.....	29
6.2 Integrated Air Sparging/Biofiltration Process.....	30
6.3 Distribution of Toluene Between Water and Sparged Air.....	38

**TABLE OF CONTENTS**  
**(Continued)**

<b>Chapter</b>	<b>Page</b>
7 CONCLUSIONS AND RECOMMENDATIONS .....	46
APPENDIX A: TOLUENE CONCENTRATION DATA FOR EXPERIMENTS: E-1 TO E-12.....	49
APPENDIX B: TOLUENE CONCENTRATION DATA FOR EXPERIMENT B .....	63
REFERENCES .....	69

## LIST OF TABLES

<b>Table</b>	<b>Page</b>
3.1 Regulations for control of toluene levels .....	17
6.1 Steady state biofiltration of toluene vapors: Experimental data .....	30
6.2 Integrated Air Sparging/Biofiltration Process: Conditions for Case Study I .....	32
6.3 Integrated Air Sparging/Biofiltration Process: Conditions for Case Study II.....	32
6.4 Integrated Air Sparging/Biofiltration Process: Conditions for Case Study III.....	33
6.5 Data from toluene distribution experiments when $V_G=1.2L$ . In all experiments an amount of 8.66mg toluene was added to 1L water.....	41
6.6 Data from toluene distribution experiments when $V_G=0.1L$ . In all experiments an amount of 8.66mg toluene was added to 1L water.....	41
6.7 Data from toluene distribution experiments when $V_G=0.1L$ and $Q_G=1.0 \times 10^{-4} m^3 min^{-1}$ . Amount of toluene added varies .....	42
6.8 Toluene distribution from an experiment with varying $Q_G$ . Toluene added: 8.6mg; $V_G=0.1L$ .....	42
6.9 Data from a toluene distribution experiment with varying $Q_G$ . Toluene added: 1.73mg; $V_G=28L$ ; $V_L=34L$ .....	44

## LIST OF FIGURES

Figure	Page
2.1 Schematic of air sparging process.....	6
2.2 Schematic layout of a biofilter .....	9
3.1 Schematic of the integrated air sparging/biofiltration process.....	14
5.1 Schematic of the unit used in the air sparging/biofiltration experiments .....	22
5.2 Schematic of the system used in toluene distribution experiments .....	24
5.3 Toluene calibration curve.....	27
6.1 Toluene concentration profiles for Case Study I. (a): at the inlet and outlet of the biofilter unit; curves 1 and 2, respectively. (b): at the exit of the tank and outlet of the biofilter; curves 1 and 2 , respectively.....	35
6.2 Toluene concentration profiles for Case Study II. (a): at the inlet and outlet of the biofilter unit; curves 1 and 2, respectively. (b): at the exit of the tank and outlet of the biofilter; curves 1 and 2 , respectively.....	36
6.3 Toluene concentration profiles for Case Study III. (a): at the inlet and outlet of the biofilter unit; curves 1 and 2, respectively. (b): at the exit of the tank and outlet of the biofilter; curves 1 and 2 , respectively.....	37
6.4 Toluene concentration data for experiment E-1 in (a): semilogarithmic and (b): arithmetic scale. Lines and curves represent regressions .....	40
6.5 Toluene concentration profile as a function of time for the three phases of experiment E-12.....	43
6.6 Toluene concentration profile as a function of time for the five phases of experiment B.....	45
A-1 Toluene concentration data for experiment E-2 in (a): semilogarithmic and (b): arithmetic scale. Lines and curves represent regressions .....	50
A-2 Toluene concentration data for experiment E-3 in (a): semilogarithmic and (b): arithmetic scale. Lines and curves represent regressions .....	51

<b>Figure</b>	<b>Page</b>
A-3 Toluene concentration data for experiment E-4 in (a): semilogarithmic and (b): arithmetic scale. Lines and curves represent regressions .....	52
A-4 Toluene concentration data for experiment E-5 in (a): semilogarithmic and (b): arithmetic scale. Lines and curves represent regressions .....	53
A-5 Toluene concentration data for experiment E-6 in (a): semilogarithmic and (b): arithmetic scale. Lines and curves represent regressions .....	54
A-6 Toluene concentration data for experiment E-7 in (a): semilogarithmic and (b): arithmetic scale. Lines and curves represent regressions .....	55
A-7 Toluene concentration data for experiment E-8 in (a): semilogarithmic and (b): arithmetic scale. Lines and curves represent regressions .....	56
A-8 Toluene concentration data for experiment E-9 in (a): semilogarithmic and (b): arithmetic scale. Lines and curves represent regressions .....	57
A-9 Toluene concentration data for experiment E-10 in (a): semilogarithmic and (b): arithmetic scale. Lines and curves represent regressions .....	58
A-10 Toluene concentration data for experiment E-11 in (a): semilogarithmic and (b): arithmetic scale. Lines and curves represent regressions .....	59
A-11 Toluene concentration data for the first phase of experiment E-12 (E-12a) in (a): semilogarithmic and (b):arithmetic scale. Lines and curves represent regressions.....	60
A-12 Toluene concentration data for the second phase of experiment E-12 (E-12b) in (a): semilogarithmic and (b):arithmetic scale. Lines and curves represent regressions.....	61
A-13 Toluene concentration data for the third phase of experiment E-12 (E-12c) in (a): semilogarithmic and (b):arithmetic scale. Lines and curves represent regressions.....	62
B-1 Toluene concentration data for the first phase of experiment B (B-1) in (a): semilogarithmic and (b):arithmetic scale. Lines and curves represent regressions.....	64
B-2 Toluene concentration data for the second phase of experiment B (B-2) in (a): semilogarithmic and (b):arithmetic scale. Lines and curves represent regressions.....	65

<b>Figure</b>	<b>Page</b>
B-3 Toluene concentration data for the third phase of experiment B (B-3) in (a): semilogarithmic and (b):arithmetic scale. Lines and curves represent regressions.....	66
B-4 Toluene concentration data for the fourth phase of experiment B (B-4) in (a): semilogarithmic and (b):arithmetic scale. Lines and curves represent regressions.....	67
B-5 Toluene concentration data for the fifth phase of experiment B (B-5) in (a): semilogarithmic and (b):arithmetic scale. Lines and curves represent regressions.....	68

## CHAPTER 1

### INTRODUCTION

During the past decade, the debate over the environment and nonrenewable resources has raised our collective consciousness about the dangers of the short-term approach. As a general proposition, we have become much more sensitive to the longer-range implications of our short-term actions. It has become apparent to most people, for example, that the short term convenience that encouraged us to pollute the air and water was not worth the long-range damage done to the quality of our lives and our environment. All the forest-products companies now have impressive reforestation programs as a result of the shared realization that if we just kept cutting down trees without replanting, few would be left for our children and grandchildren (13).

Soil and groundwater contamination by volatile organic chemicals (VOCs) has become a major environmental problem in many industrialized countries. These contaminants are introduced into the subsurface as a result of accidental surface spills, leakage from underground storage tanks, or waste disposal. In general, VOCs are highly toxic and water soluble, and their presence in soils poses a serious threat to groundwater. In recent years, several *in situ* remediation techniques have been developed for soil and groundwater contaminated by VOCs, including biological degradation, vapor extraction, steam stripping, vitrification, supercritical solvent extraction, low temperature thermal desorption, and radio frequency heating.



The first step in most remediation projects is to remove free-phase contamination from the groundwater surface. This involves the installation of recovery wells and pumps. Contaminated groundwater, removed by a water table depression pump, is pumped to a treatment unit (usually an air stripper) to remove dissolved hydrocarbon contaminants prior to discharge or recharge to the subsurface. The pumping and treating method effectively removes free- and dissolved phase petroleum contamination, but it is not the answer to site remediation. It does not remove the source of continued contamination, the adsorbed phase product, which dissolves into the groundwater when the water percolates through the soil. However, in the past four years, a volatilization technology for adsorbed and dissolved contamination in the saturated zone has been commercialized. Known as air sparging, this method involves highly controlled injection of air under pressure into the saturated zone. Used with venting, it can reduce the cost and project life cycle of many fuel and lubricant remediation projects. However, because this air-based primary treatment technology is relatively new, sparging is not now included in the RAPs (Remedial Action Plans) for most military sites.

Usually, the adsorbed and dissolved contamination that is removed to the surface is directly discharged to the air (where permitted) or it is treated by catalytic conversion or carbon adsorption. The present study investigates the biofiltration process as an alternate approach to treat the air that is brought to the surface after it is sparged through contaminated groundwater and soils.

There are a lot of technologies for removing contamination from one or more of the contaminated phases, in which the pollutants are distributed, but none is applicable to all

phases. Therefore, the most complete and effective systems are combinations of mutually compatible and supportive treatment technologies in which the strengths of some offset weaknesses in others.

The results of using combined technologies is a better process efficiency and a lower operation cost. The Air sparging/Biofiltration process is a different approach to removing dissolved pollutants. Air can be used for decontaminating a soil or an aquifer contaminated with VOCs, removing the pollutant to the air. This contaminated air could be subsequently treated in a biofilter where the pollutants are destroyed.

The use of the two technologies is constrained to the biofilter operation conditions. The biofilter is designed to operate at a certain residence time and (usually) with a constant inlet concentration. The main idea of integrating air sparging and biofiltration, which is examined here, is based on the premise that the use of different flow rates for the sparged air and dilutions of it with uncontaminated air, can lead to the proper operating conditions (inlet concentration and air flow) for the biofilter.

This study intended to show experimentally, that continuous biofilter operation is feasible under constant air flow rate and variation of the air flow through contaminated groundwater. As part of this effort, independent experiments were performed in order to understand the distribution of a pollutant (toluene was used as model compound) between groundwater and sparged air. It is important to mention that all final conditions selected for demonstration, complied with the Threshold Limit Value (TLV), Acceptable Source Impact (ASIL) and Action Level in Groundwater for the pollutant of interest. These concepts will be discussed in the following chapters.

## CHAPTER 2

### LITERATURE REVIEW

#### 2.1 Multiphase Contamination

A prerequisite for selecting the most cost-effective combination of remediation technologies is an understanding of how contamination is distributed in the ground subsurface. Chemicals can enter the ground because of accidents, leaking tanks, pipes, valves, drainage systems, and the improper disposal of waste products. Pollutants travel horizontally and vertically through the soil, forming a cone-shaped plume extending to the groundwater. When contaminants reach the water table, the soluble components dissolve into the groundwater and the rest typically float on the water table. Heavier than water contaminants, such as chlorinated solvents, continue to migrate down through the groundwater until they reach clay, bedrock, or some other impermeable geologic stratum.

Subsurface contamination is said to exist in four phases. Separate -or free- phase contamination floats on the top of the groundwater or at the bottom of the formation; contaminants adhering to the soil form the adsorbed phase; soluble contaminants in the groundwater form the dissolved phase; vapors that are in, or migrate through, the unsaturated soil constitute the vapor phase. All four phases are interrelated. Seasonal or tidal fluctuations in groundwater levels can “smear” free-phase contamination in the groundwater fluctuation zone to create more adsorbed phase contamination. At the same time, adsorbed and separate-phase contamination contribute to the dissolved phase. The vapor phase is usually a product of the adsorbed-phase contamination as it is generated by

air moving through the soil. Because of these interrelationships, treating only one phase will rarely stabilize the site at acceptable levels (7).

Complete decontamination usually requires the use of a combination of various technologies as no technology capable of effectively treating multiphase contamination exists. Individual technologies of interest for the work presented here are air sparging and biofiltration, and they are reviewed in the next sections.

## 2.2 Air Sparging

Air sparging is the highly controlled injection of air into a contaminated saturated zone (see Figure 2.1). Air bubbles traverse horizontally and vertically through the soil, creating a transient air filled zone in which volatilization can occur. Air sparging creates a crude air stripper in the subsurface. Air bubbles that contact dissolved and adsorbed-phase contaminants in the aquifer cause the VOCs to volatilize. The entrained organics are carried by the bubbles into the vadose zone to be captured by a vapor extraction system or where permissible, to escape through the ground surface (9).

Although air sparging is simple in concept and can, in principle, effectively remove pollutants from groundwater and soil, there are two main reservations regarding its use. The first, refers to the accelerated vapor travel created by sparging which can lead to the potential for vapors to be drawn into nearby receptors such as basements. This problem, however, can be resolved by using venting systems in areas with potential vapors receptors. The second concern is that, under specific conditions, a misapplied sparge system could push the contamination plume down-gradient. For example, a clay barrier above the

injection zone could allow this to happen. Down-gradient flow could also be caused by pressurization of the system beyond the capacity of the soil to accept a smooth flow of injected air. Therefore, restrictive geological conditions and system operating pressures must be determined by meticulous tests before air sparging is implemented. If barriers and low permeable formations are found, groundwater recovery may be necessary to prevent the spread of dissolved contamination (8). Furthermore, air sparging has demonstrated sensitivity to minute soil permeability changes, which can result in localized stripping between the sparged and monitoring wells.

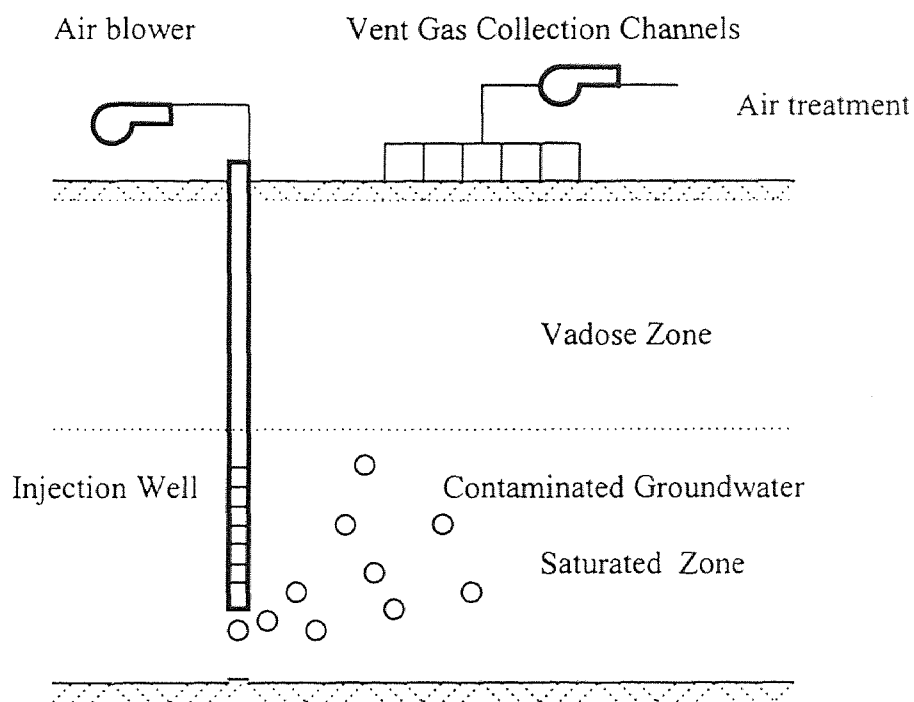


**Figure 2.1** Schematic of air sparging process

A pilot scale field study was conducted at the Amoco Production Company Kalkaska Gas Processing Plant (KGPP) near Kalkaska, Michigan in 1993 (2), to assess the

efficacy of utilizing *in situ* air sparging to remediate subsurface BTEX contamination in the aquifer and vadose zone. Some of the goals of this investigation, which are of interest to the present study, were to evaluate the potential for enhancing the removal of dissolved BTEX contaminants in the groundwater by sparging air into the aquifer; determine if sparging air into the aquifer enhanced partitioning of BTEX dissolved in groundwater into the advective gas phase with subsequent transport to the vadose zone; evaluate the potential for BTEX in the advective gas phase to be volatilized to the atmosphere and determine if *in situ* air sparging causes significant downward or lateral dispersion of BTEX in the aquifer. The results showed that injecting air into the saturated zone facilitated the volatilization of VOCs (BTEX) dissolved in groundwater and sorbed to the soil. The volatiles were released to the advective air phase and migrated into the vadose zone where they were presumably degraded by indigenous microbes. BTEX compounds were not volatilized at the surface during active air sparging.

During the past decade, petroleum-contaminated soils and groundwater at military bases have been carefully assessed and documented. It has been reported (7) that air sparging is being implemented in some of these military bases. However, because this air-based primary treatment technology is relatively new, sparging is not now included in the RAPs (Remedial Action Plans) for most military sites.

During air sparging, as it was mentioned above, VOCs dissolved in groundwater are transported to the vadose zone. Extraction wells screened in the vadose zone are typically utilized to extract the VOCs from the ground for treatment at the surface. However, treatment at the surface often involves expensive equipment to control air

emissions. Also, air discharge permits often have to be obtained from appropriate regulatory bodies.

Biofiltration is a relatively new control technology used in the treatment of contaminated gas streams. Due to its efficiency and its economical advantage over other expensive off-gas treatment methods, it represents a good alternative to combine with the air sparging process. Biofiltration is discussed in the next section.

### **2.3 Biofiltration**

Biofiltration is a technology in which vapor-phase organic contaminants are passed through a bed of solids and are degraded by microorganisms present on the surface of these solids. Specific strains of bacteria may be introduced into the filter and optimal conditions can be selected to preferentially degrade specific compounds. Biofilters provide several advantages over conventional activated carbon adsorbers. First, bioregeneration keeps the maximum adsorption capacity available constantly. The filter does not require regeneration, and the required bed length is greatly reduced. These features reduce capital cost and operating expenses. Additionally, the contaminants are destroyed, not just removed into another phase (16).

There are two types of biofilters: classical or conventional biofilters and biotrickling filters. This thesis involves the study of a classical biofilter, which is schematically shown in Figure 2.2. Classical biofilters utilize porous solid particles (15) of an organic base (e.g. peat moss, compost, bark, etc.) as a substratum for the formation of layers of microorganisms. The pores of the solids are partially filled with water, thus providing the

necessary moisture for microbial activity. They do not involve a continuous liquid (water) phase and require complete humidification of the polluted airstream before it enters the biofilter bed. Classical biofilters are open or closed structures containing the solids. Closed structures are easier to control. Classical biofilters are packed-bed vapor phase biological reactors. Their operation is relatively simple, requires no engineering attendance, and its cost appears to be low (19). Biotrickling filters are always closed structures containing non-porous particles of an inorganic base (plastics, ceramics) as a substratum for the formation of biofilms (6). They employ a continuous liquid phase which trickles through the bed of solids. The liquid phase is primarily water which also contains various nutrients other than carbon/energy sources for the microorganisms (e.g. sources of nitrogen, phosphorus, vitamins, etc.) They lead to the formation of substantial amounts of biomass which need to periodically be removed from the filter-bed. Biotrickling filters also allow for good pH-control and seem to be ideal in cases of treatment of chlorinated VOCs.

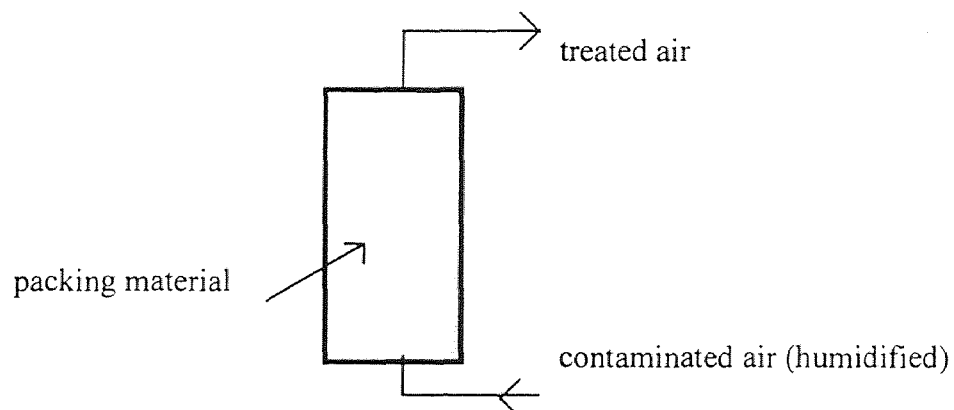


**Figure 2.2** Schematic layout of a conventional biofilter



There are different ways to inoculate a conventional biofilter. Naturally occurring packing materials such as peat and compost, contain organisms capable of biodegrading some VOCs. Poorly biodegradable compounds such as chlorinated hydrocarbons (e.g. dichloromethane, vinyl chloride), and aromatics (e.g., benzene, toluene), require inoculation with specially cultivated organisms (16).

Most researchers in the United States have shifted their interests towards the development of biotrickling filters, although it is not yet clear whether they have an unconditional advantage over classical biofilters (17).

As with any biological treatment process, biofiltration is highly dependent upon the biodegradability of the contaminants. Under proper conditions, biofilters can remove virtually all selected contaminants to harmless products. Conventional biofiltration is used primarily to treat nonhalogenated VOCs and fuel hydrocarbons. Halogenated VOCs can also be treated, but the process may be less effective. Biofilters have been successfully used to control odors from compost piles (8).

There are many factors that can affect the performance of a biofilter. Moisture and temperature effects may create serious problems for the biofiltration process if they are not properly controlled. Water is required for biological activity, and is retained in the biolayer and the pore structure of the packing material. According to some studies (20), the optimal operation of a biofilter is reached when 50% of the pores are filled with water. It is important to humidify the contaminated airstreams before they are supplied to the biofilter, since biofiltration is a process involving exothermic reactions, and their heat may dry the packing (17).

Regarding temperatures of operation for biofilter units, it has been reported that they should be between 5 and 50°C (3). Over certain temperature ranges, one could use an Arrhenius expression to describe the effect of temperature on biodegradation, and consequently on biofiltration (20).

The pressure drop in a biofilter is very low (5). Typical values are around 1 to 2" water/m-filter-bed (5). Pressure drop increases have been observed in cases where a sprinkling system is used for water addition (16), and are due to the fact that excess water at the top of the biofilter leads to clogging of the packing material.

Maintenance of proper pH levels in trickling bed configuration units is very important when chlorinated solvents and nitroaromatic compounds are removed from airstreams by biofiltration. In case of simple solvents such ethanol, problems with the pH may arise only when acid is produced due to oxygen availability problems (10). In such cases, incomplete mineralization of the pollutant occurs and the problem is not so much related with pH as with the proper supply of oxygen to the unit.

Although, the objective of the present work was to study the integrated air sparging/biofiltration process as a whole, it is important to mention that there have been several studies on biofiltration alone and thus, this part of the process is relatively well understood.

The first studies on biofiltration involved removal of single VOCs from airstreams. It has been demonstrated that a wide range of pollutants can be effectively degraded using biofiltration (4). A feasibility study on phenol removal in a biofilter using cultures belonging to the *Pseudomonas* genus, for example, (20) led to a high degradation of this

pollutant. Based on these kind of studies and the necessity to describe and predict the behavior of biofilters mathematically, the first model of biofiltration under steady-state conditions was developed by Ottengraf and van den Oever (14). This model did not take into consideration several factors that affect the performance of a biofilter, such as oxygen availability and kinetic interactions between pollutants (18). Later on, a more detailed model under steady-state conditions was developed (18). This model considered potential oxygen limitations of the process and was validated experimentally through the use of methanol as a model compound. The results obtained show that, under most conditions, oxygen is the limiting factor from the mass transfer point of view while the carbon source (methanol) is the limiting factor from the kinetics point of view (18). Other studies with ethanol and butanol in separate units (1) and benzene and toluene (17) using the same model, led to the same conclusions regarding oxygen limitation.

Another mathematical model was proposed to describe transient behavior of single VOC removal in biofilters and was experimentally validated with toluene as model compound (17). This transient model takes into account adsorption/desorption effects which are most important when discussing transient biofilter behavior. Since the present study involved air sparging and biofiltration, the biofilter is expected to operate under transient conditions. To alleviate adverse effects of desorption on the integrated process, special care needs to be taken so that concentration fluctuations are minimized. This is an issue discussed in a subsequent chapter.

There are some studies involving the use of biofilters to treat volatile organic compounds removed from aquifers and soils. It has been reported (12) that an integrated

soil vapor extraction/biofiltration process was implemented at a gasoline contaminated site and led to a 43% hydrocarbon removal. Other studies (11) using a soil vapor extraction/biofiltration process at two gasoline service stations reported that the process is efficient for aromatic hydrocarbons but yields relatively poor results for aliphatic compounds.

No detailed studies on air sparging/biofiltration were found in the literature regarding experimental evidence of process feasibility and/or performance. Two modeling studies (4, 19) have dealt with the process considered in this thesis. These studies predict that proper process design can lead to groundwater cleaning under conditions meeting all environmental regulatory constraints. In this thesis the main focus was on experimentally showing that theoretical predictions are correct.

## CHAPTER 3

### OBJECTIVES

The objectives of the present study can be easier discussed when the schematic of Figure 3.1 is considered.

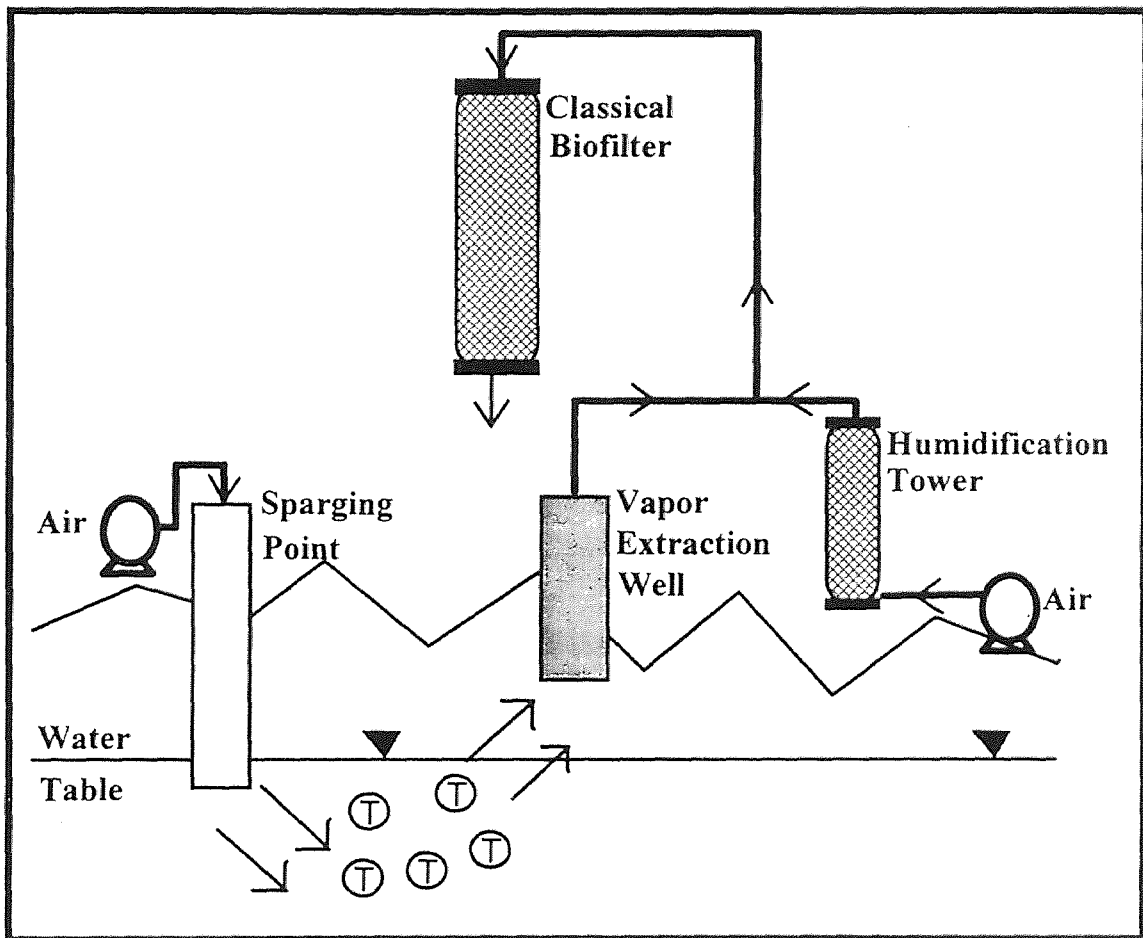


**Figure 3.1** Schematic of the integrated air sparging/biofiltration process

The schematic above, originally proposed by Cohen (4) and Stamatiadis (19), is a conceptual drawing for the integrated air sparging/biofiltration process. The idea is that a

contaminated aquifer (groundwater) is sparged with air in order to volatilize the dissolved pollutants. This way, pollution is transferred from the water (liquid phase) to the air (gas phase). Subsequently, the contaminated air is treated in a biofilter. Overall, the concept is that the air is an intermediary for an *ex-situ* biodegradation of the pollutants present in the groundwater. The design of such a process requires that the biofilter operates under relatively constant pollutant concentrations and in order to achieve this, it has been proposed (4, 19) that the air extracted from the aquifer is diluted with pure air as shown in Figure 3.1.

If  $Q_1$  and  $Q_2$  are the flow rates of air through the aquifer and the clean air used for diluting the extracted air, earlier work of Cohen (4) and Stamatiadis (19) has shown through the computer calculations that by manipulating the relative values of  $Q_1$  and  $Q_2$  over time, while keeping  $Q_1 + Q_2$  constant, one can have an acceptable design and successful operation of the integrated process. Earlier results were only computational and thus, the main objective of the present thesis was to experimentally demonstrate that the predicted process behavior can in fact be observed.

In order to meet the objective above, an existing biofilter was used and was connected to a specially designed 65 liter vessel in which water was placed to simulate the contaminated aquifer. Both, the biofilter and the water tank are described in Chapter 5.

Toluene was used as model compound for the experiments. Selection of the compound was based on two reasons: the existing biofilter was operated with toluene vapor and the properties (kinetics, etc.) of toluene had been used in the calculations of Cohen (4) and Stamatiadis (19) for the integrated air sparging/biofiltration process.

The intent of the experiments was not only to show that the integrated process works, but also show that specific subobjectives can be also met. These, also discussed elsewhere (4, 19), are the following.

1. The concentration of toluene in the aquifer at the end of the remediation operation should be at, or below, the toluene Action Level in Groundwater as per existing regulations (see Table 3.1).
2. The concentration of toluene in the air exiting the extraction wells should be very close to the Threshold Limit Value (TLV) as per existing regulations (see Table 3.1).  
The American Conference of Governmental Industrial Hygienists (ACGIH) has established threshold doses called threshold limit values (TLVs) for a large number of chemical agents. The TLV refers to airborne concentrations that correspond to conditions where no adverse effects are normally expected during a worker's life time. The TLV was formerly called the maximum allowable concentration (MAC).
3. The concentration of toluene at the exit of the biofilter should meet the Acceptable Source Impact Level (ASIL) as per existing regulations (see Table 3.1).
4. The biofilter should be exposed to relatively constant toluene concentrations over the majority of the remediation operation.

It should be mentioned here that earlier studies (4, 19) assumed a given level of aquifer contamination, a given value for the total air flow rate through the biofilter and calculated the volume of biofilter bed required to meet the design criteria discussed above. Here, the problem was essentially reversed. Since the biofilter volume was given (existing unit used), the total air flow rate had to be experimentally determined and then

**Table 3.1** Regulations for control of toluene levels [taken from reference (4)]

<b>Parameter</b>	<b>Value</b>	<b>Units</b>
Threshold Limit Value (TLV) <sup>a</sup>	86.69	g/m <sup>3</sup>
Acceptable Source Impact Level (ASIL) <sup>b</sup>	0.2817	g/m <sup>3</sup>
Action Level in Groundwater <sup>c</sup>	1.0	g/m <sup>3</sup>

<sup>a</sup> TLV established by American Conference of Governmental Industrial Hygienist (1993).

<sup>b</sup> ASIL established by the Washington State Department of Ecology (1994).

<sup>c</sup> Action Level established in 40CFR131 of Federal Register (1993).

used to demonstrate that the design criteria above, can be actually, experimentally, met.

Cohen (4) in his calculations assumed that the pollutant (toluene) is always in equilibrium distribution between the groundwater and the air sparged through it. Stamatiadis (19) considered cases where the distribution was not as dictated by thermodynamic equilibrium, but assumed a constant deviation from equilibrium in all cases he investigated. There is not experimental evidence about pollutant distribution between water and air sparged through it and for this reason, the second main objective of this thesis was to perform small scale experiments and determine the distribution of a pollutant (toluene was used as model compound) between water and sparged air as a function of the volumetric flow rate of air used for sparging.

From the foregoing discussion it becomes clear that the objectives of the present work were:

- I. To experimentally show that an integrated air sparging/biofiltration process can work and meet criteria and restrictions imposed by existing environmental regulations.



- II. To experimentally find the distribution of a pollutant present in an aquifer between groundwater and air sparged through the aquifer as a function of air flow rate.

## CHAPTER 4

### DESCRIPTION OF POLLUTANT DISTRIBUTION BETWEEN WATER AND SPARGED AIR

Consider a closed vessel of volume  $V$  where an amount of water of volume  $V_L$  is placed. The difference between  $V$  and  $V_L$  is  $V_G$ , i.e. the volume of the air (headspace) in the vessel. Assume that an amount  $M$  of a pollutant is present in the vessel and distributed between the liquid and air. If the pollutant does not adsorb onto the walls of the vessel, and if the vessel is completely closed one has the following relationship:

$$M = V_L c_L(t) + V_G c_G(t) \quad (4.1)$$

where  $c_L$  and  $c_G$  are the pollutant concentrations in the liquid and gas phase, respectively. The equation above assumes that  $M$  is not excessively high and thus, no non-aqueous phase liquid (NAPL) is present in the vessel. If one waits long enough, equilibrium distribution of the pollutant between water and air is achieved and, if Henry's law is valid, one has

$$c_G = m c_L \quad (4.2)$$

where  $m$  is the dimensionless Henry constant for the pollutant.

If equilibrium has been reached, the concentrations appearing in equation (4.1) are not functions of time and are interrelated as dictated by equation (4.2)

If equilibrium distribution has not yet been reached, one could write the following equation

$$c_G(t) = m\sigma(t)c_L(t) \quad (4.3)$$

where  $\sigma(t)$  is a function describing deviation from equilibrium. As the time passes, one expects that  $\sigma$  becomes constant and equal to 1 (equilibrium).

Assume now that completely humidified air is sparged through the water and then collected at the exit of the vessel. Assuming that the concentration of the pollutant in the exiting air is  $c_G(t)$ , i.e., same as the concentration in the headspace of the vessel, and that the volumetric flow rate of the air is  $Q$  one can write the following mass balance:

$$\frac{dM}{dt} = -Qc_G \quad (4.4)$$

Using equations (4.1) and (4.4) one can get:

$$V_L \frac{dc_L}{dt} + V_G \frac{dc_G}{dt} = -Qc_G \quad (4.5)$$

For the case where air is sparged through the water one can assume that equation (4.3) is valid with a constant  $\sigma$  where  $\sigma$  now incorporates mass transfer effects. In this case, one gets from (4.5) that

$$(V_L + m\sigma V_G) \frac{dc_L}{dt} = -Qm\sigma c_L \quad (4.6)$$

which upon integration subject to the initial condition that at  $t = 0$ :  $c_L = c_{L_0}$ , leads to,

$$c_L = c_{L_0} e^{-bt} \quad (4.7)$$

where,

$$b = \frac{Q\sigma m}{V_L + m\sigma V_G} \quad (4.8)$$

Using equation (4.7) and equation (4.3) with  $\sigma$  being constant one gets

$$c_G = m\sigma c_{L_0} e^{-bt} \quad (4.9)$$

Taking the natural logarithm of equation (4.9) one gets

$$\ln c_G = K - bt \quad (4.10)$$

where,

$$K = \ln(m\sigma c_{L_0}) \quad (4.11)$$

Equation (4.10) suggests that a semilogarithmic plot of  $c_G(t)$  data versus  $t$  should lead to a straight line of intercept  $K$  and slope equal to  $-b$ . Knowing the value of  $b$  and the values of  $Q$ ,  $V_L$ ,  $V_G$ , and  $m$  one can calculate the value of  $\sigma$  from equation (4.8), as

$$\sigma = \frac{bV_L}{m(Q - bV_G)} \quad (4.12)$$

Knowing the values of  $\sigma$  [via (4.12)], the intercept  $K$ , and  $m$ , the value of  $c_{L_0}$  can be calculated via equation (4.11) as,

$$c_{L_0} = \frac{e^K}{\sigma m} \quad (4.13)$$

If the value of  $c_{L_0}$  is known, it should then match the one predicted by equation (4.13). It should be mentioned though that, experimentally, it is easier to measure  $c_{G_0}$  rather than  $c_{L_0}$ . Knowing the value of  $c_{G_0}$  one could predict the  $c_{L_0}$  value via equation (4.3). However, the following should be kept in mind. At  $t = 0$  (time when air sparging begins) the distribution of the pollutant between water and air may be different from the distribution during air sparging. For example, if air sparging begins a long time after water with dissolved pollutant have been placed in the closed vessel one expects to have  $\sigma = 1$ . Thus, regression of all data to equation (4.9) may be problematic. Better results can be obtained if the initial data are neglected. This means that  $c_{L_0}$  may not be necessarily be known.

## CHAPTER 5

### EXPERIMENTAL APPROACH AND PROCEDURES

#### 5.1 Apparatus for the Air Sparging/Biofiltration Studies

A schematic of the unit used in the air sparging/biofiltration experiments is shown in Figure 5.1

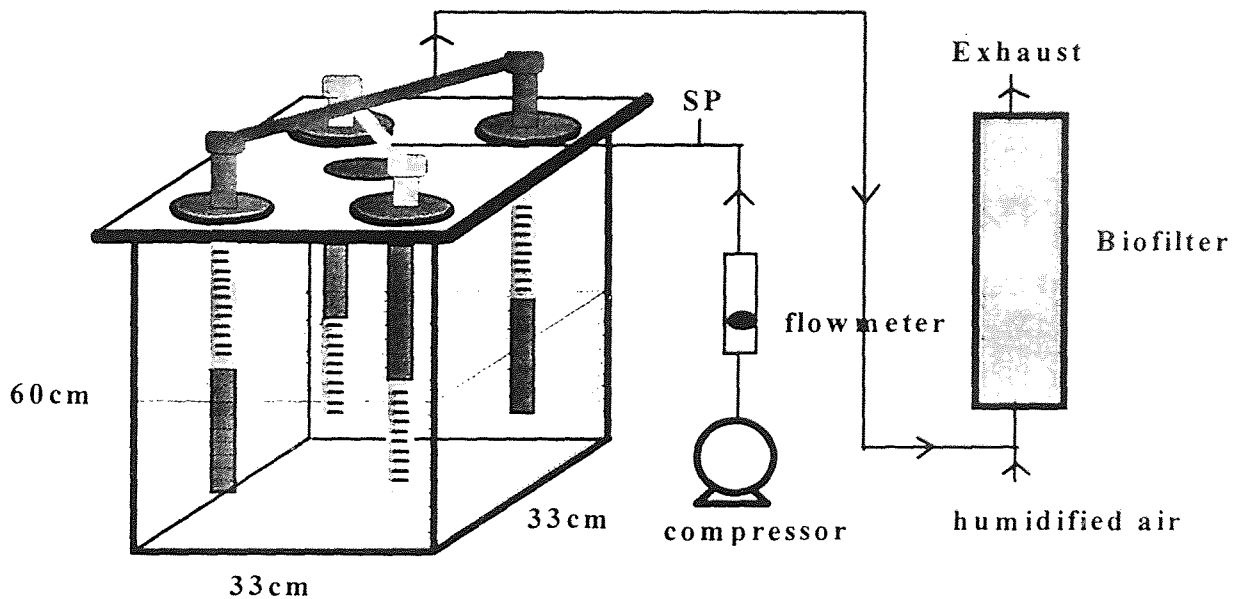


**Figure 5.1** Schematic of the unit used in the air sparging/biofiltration experiments

The schematic shows details of the vessel used in simulating the contaminated aquifer. This was a custom made (Grewe Plastics, Inc., Newark, NJ) plexiglass structure having a square (33cm x 33cm) cross section and a height of 60 cm. The lid of the vessel had five ports, one at the center which was never used and four symmetrically placed ones through which PVC pipes were placed vertically into the vessel. The PVC pipes had a diameter of 1.905cm and were perforated creating screens of 0.025cm. These pipes

were purchased from Morris Industries, Inc (Pompton Plains, NJ). The pipes were attached to the lid of the vessel with PVC flanges (McMaster-Carr Supply Co., New Brunswick, NJ) The four pipes were connected at their parts in the atmosphere forming two pairs. Each pair had pipes placed diagonally in the vessel. The, external, connecting pipes were made of PVC and had a diameter of 1.905cm (McMaster-Carr Supply Co., New Brunswick, NJ) Air was supplied to the tank through one of the two vertical PVC pipes pairs. To ensure that all air was sparged through the water, the upper part of the screens was masked with teflon tape (Fisher Scientific, Springfield, NJ). Air was coming out of the vessel through the other pair of diagonally placed PVC vertical pipes. In this case, the lower part of the screens (the ones present in the water) were masked with teflon tape so that all air was drawn from the head space of the tank.

Air was supplied to the tank through the use of a compressor and its flow was regulated through a flow meter (Matheson Inc, Morris Plains, NJ). The air exiting the tank was mixed with a prehumidified airstream and then supplied to the biofilter shown in Figure 5.1.

Details of the biofilter unit are not given here since it was a pre-existing unit used and described by Shareefdeen (17). Briefly, it was a glass column consisting of three equal segments connected in series. Each segment had a height of 30.5cm and a diameter of 15.2cm. Although the column was provided with sample ports at the end of each segment, during experiments the toluene concentration was measured only in the air entering and exiting the biofilter. Additionally, the toluene concentration in the air stream exiting the tank (after sparging through groundwater) was also monitored.

The biofilter unit was packed with a 2:3 (volume ratio) mixture of peatmoss and perlite and had been prepared according to the methodology described by Shareefdeen (17). Only one part (segment) of the packing material had to be replaced during the experiments reported here. Replacement followed exactly the steps, materials and methods described elsewhere (17).

## 5.2 Apparatus for the Toluene Distribution Experiments

The apparatus used in the experiments for determining the toluene distribution between water and air sparged through the water is shown schematically in Figure 5.2.

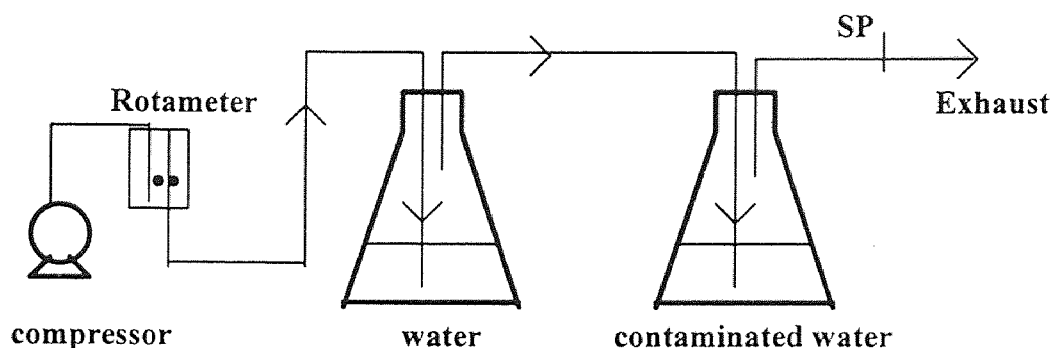


**Figure 5.2** Schematic of the system used in the toluene distribution experiments

Primarily, the unit consisted of two Erlenmeyer flasks connected in series. The first had a 1.1L volume while the second had a volume of either 2.2L or 1.1L depending on the experiment. Air from a compressor was regulated through the use of a rotameter assembly (model 75-350, Gow-Mac Instrument Co., Bound Brook, NJ) and first passed through a flask containing deionized water. This was done in order to humidify the air stream before it was passed through the flask containing a water solution of toluene. Humidification of the air allowed the volume of the water in the second flask to remain constant during the experiments. The second flask was closed with a teflon stopper. Air exiting the second flask was analyzed for toluene presence.

### 5.3 Materials

The main material used in the present study was toluene (T289-4, Certified, Fisher Scientific, Springfield, NJ). Deionized water was used for preparing toluene solutions and for humidifying airstreams.

A segment of the biofilter unit needed replacement during the course of this study. This was necessary due to inactivity probably caused by drying of the packing. Replacement required cultivating the microbial consortium from an inoculum, preparation and usage of culture media, autoclaving the peatmoss, etc. This is a lengthy and time consuming procedure during which a large number of chemicals is used. Since the chemicals and the recipes were identical with those described by Shareefdeen (17), they are not repeated here.

### 5.4 Analytical

The present study required measurement of toluene concentrations in airstreams. This was done by using a Hewlett-Packard Model 5890 (series II, Hewlett-Packard, Paramus, NJ) gas chromatograph equipped with a 6'x1/5" stainless steel column packed with 5%SP-1200/ 5% Bentone 34 on 100/120 Supelcoport packing (Supelco, Inc., Bellefonte, PA), and a flame ionization detector. Operating conditions were: injector 120°C, oven 90°C, detector 200°C, carrier gas (N<sub>2</sub>) 20.4 mL/min. Under these conditions, the retention time of toluene was 3.0 min. The calibration curve was prepared as follows. First, known volumes or precise amounts of toluene were injected into several serum bottles (160 mL)



using a 10 $\mu$ L liquid syringe (14-824, Fisher Scientific, Springfield, NJ). The bottles were closed with teflon-faced silicon septa and aluminum crimp caps. The toluene was allowed to evaporate completely at room temperature within the enclosed space. Subsequently, air samples were taken from the bottles with a gas-tight, 0.5mL pressure-LOK<sup>®</sup> syringe (Precision Sampling Corp., Baton Rouge, Louisiana), and injected to the GC. During all experiments, the same type of gas-tight syringes were used for obtaining air samples from various ports of the apparatus. These samples were subjected to GC analysis, and concentrations were read from the calibration curve. GC calibration was repeated every two to three weeks. A sample is shown in Figure 5.3.

### **5.5 Procedures for the Air Sparging/Biofiltration Experiments**

Experiments with the unit shown in Figure 5.1 were performed as follows. Initially, the water tank was not connected to the biofilter. The water tank was opened and an amount of water (approximately 32L) was placed in it so that the tank was half-full. Subsequently, an amount of (liquid) toluene was added to the water, the vessel was closed, shaken and left over night. The next day, the tank was connected to the biofilter and air was sparged through the tank. The volumetric flow rate of air used in sparging the water was varied during the course of the experiment. Similarly, the flow rate of the prehumidified airstream was also varied. However, the total air flow rate through the biofilter was kept constant at a value determined as discussed in Chapter 6.

Each experiment lasted for a period of 8-10 hours till the concentration of toluene exiting the tank reached very low levels (see results in Chapter 6). During each

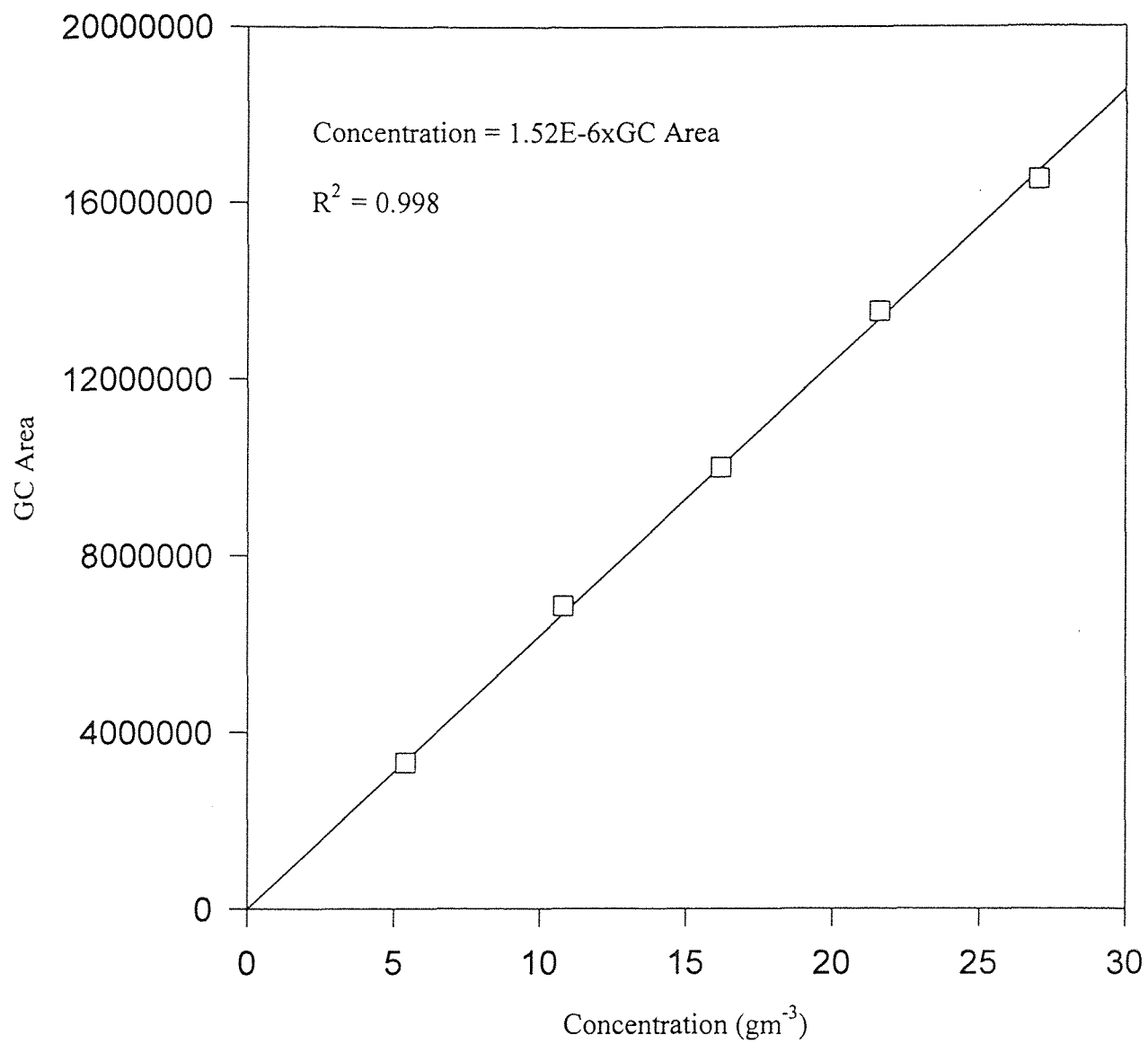


Figure 5.3 Toluene calibration curve

experiment, toluene concentration profiles were obtained at the entrance and exit of the biofilter via GC analysis of samples taken every 12 min from each sampling location.

When the water tank was not connected to the biofilter, the biofilter was still supplied with air carrying low toluene concentrations in order to ensure that its activity was maintained. In some occasions, amounts of nutrient media (17) were added to the biofilter primarily for moisture control purposes. These instances were rare and did not lead to any significant change in the biofilter performance.

### **5.6 Procedures for the Toluene Distribution Experiments**

In the second flask of the apparatus shown in Figure 5.2 one liter of water was placed. An amount of toluene was placed in it. The flask was shaken and allowed to equilibrate for about 3 hours. In some experiments (those with 2.2L flasks) no equilibration period was allowed. Air was passed through the system (after the equilibration period, if there was one) and the toluene presence in the air exiting the second flask was monitored via GC analysis of samples. The amount of toluene added to the water as well as the volumetric flow rate of the air varied between experiments. Each experiment lasted for a period of about 3 hours.

## CHAPTER 6

### RESULTS AND DISCUSSION

#### 6.1 Preliminary Biofilter Experiments

As discussed in Chapter 4 one of the main objectives of the present study was to experimentally demonstrate that an integrated air sparging/biofiltration process works and can be designed to meet environmental criteria such as ASIL, etc. Since an existing biofilter unit was to be used, as discussed in Chapter 5, the first experiments entailed finding the space time ( $\tau$ ) of the air in the biofilter bed and the toluene concentration at the inlet of the biofilter ( $C_{Ti}$ ) which, with the existing unit, could lead to concentrations of toluene at the biofilter exit ( $C_{Te}$ ) meeting the ASIL criterion (see Table 3.1).

These experiments were performed with the biofilter in the same way as those reported by Shareefdeen (17). Results from these experiments are shown in Table 6.1. In addition to the  $\tau$ ,  $C_{Ti}$  and  $C_{Te}$  values, the table shows the percent removal ( $X$ ) of toluene achieved, the load to the biofilter ( $L = C_{Ti}/\tau$ ) and the removal rate of toluene obtained [ $R = (C_{Ti}-C_{Te})/\tau$ ].

All  $C_{Te}$  values reported in Table 6.1 meet the ASIL constraint. For this to happen, a number of ( $\tau$ ,  $C_{Ti}$ ) pair values exist. The lower  $\tau$  is the lower must be the  $C_{Ti}$  value. It was finally decided to do experiments with a  $C_{Ti}$  value not exceeding  $1\text{gm}^{-3}$  and thus, in order to ensure meeting the ASIL criterion at all times, a  $\tau$  of 6.6min was selected. Since  $\tau = V_p/F$ , with  $V_p$  and  $F$  being the volume of biofilter packing material and the flow rate

**Table 6.1** Steady state biofiltration of toluene vapors: Experimental data

$\tau$ (min)	$C_{Ti}$ ( $gm^{-3}$ )	$C_{Te}$ ( $gm^{-3}$ )	X %	L ( $gm^{-3}$ -packing $h^{-1}$ )	R
2.7	0.54	0.25	53.4	12.1	6.4
4.1	0.89	0.27	69.2	13.0	9.1
6.6	1.02	0.26	74.5	9.3	6.9

$\tau$ : residence time;  $C_{Ti}$ : inlet toluene concentration;  $C_{Te}$ : exit toluene concentration; X percent removal defined as  $100 \times (C_{Ti} - C_{Te}) / C_{Ti}$ ; R: removal rate; L: load.

the air supplied to the biofilter, respectively, and since the  $V_p$  of the existing unit was fixed ( $0.0166m^3$ ), selection of  $\tau$  implied selection of  $F$ . In fact, a value of  $2.5 \times 10^{-3} m^3 min^{-1}$  was used in all experiments.

With the value of  $F$  decided from these preliminary experiments, the intent of the subsequent air sparging/biofiltration experiments was to select the values for the flow rate of air sparged through the groundwater and that of the prehumidified air (see Figure 5.1) so that the biofilter operates with air having  $F = 2.5 \times 10^{-3} m^3 min^{-1}$ , meets ASIL levels at its exit, and the toluene levels in all air lines is well below the TLV regulations (see Table 3.1).

## 6.2 Integrated Air Sparging/Biofiltration Process

Three case studies are reported here for the integrated process. The conditions are given in Tables 6.2 through 6.4 while toluene concentration profiles at the entrance and exit of the biofilter and the exit of the tank (see Figure 5.1) are shown in Figures 6.1 through 6.3.

**Table 6.2** Integrated Air Sparging/Biofiltration Process. Conditions for Case Study I

time (min)	$Q_G$ ( $m^3 min^{-1}$ )	$F_d$ ( $m^3 min^{-1}$ )	M (g)
182.82	$2.0 \times 10^{-4}$	$2.3 \times 10^{-3}$	0.36
243.73	$4.0 \times 10^{-4}$	$2.1 \times 10^{-3}$	0.12
281.02	$8.0 \times 10^{-4}$	$1.7 \times 10^{-3}$	0.06
366.32	$1.6 \times 10^{-3}$	$9.0 \times 10^{-4}$	0.14
521.85	$2.5 \times 10^{-3}$	0.0	0.94

$Q_G$  : flow rate of air entering the sparging point;  $F_c$  : flow rate of the clean air used to dilute the contaminated air stream; M : mass recovered during the time period indicated;  $C_{L0}=50.94g/m^3$ ; Amount of toluene recovered : 94.28% of that added.

**Table 6.3** Integrated Air Sparging/Biofiltration Process. Conditions for Case Study II

time (min)	$Q_G$ ( $m^3 min^{-1}$ )	$F_d$ ( $m^3 min^{-1}$ )	M (g)
175.33	$2.0 \times 10^{-4}$	$2.3 \times 10^{-3}$	0.35
238.35	$3.0 \times 10^{-4}$	$2.2 \times 10^{-3}$	0.11
291.53	$6.0 \times 10^{-4}$	$1.9 \times 10^{-3}$	0.10
335.30	$1.0 \times 10^{-3}$	$1.5 \times 10^{-3}$	0.07
529.78	$1.5 \times 10^{-3}$	$1.0 \times 10^{-3}$	0.34
584.95	$2.0 \times 10^{-3}$	$5.0 \times 10^{-4}$	0.09
641.75	$2.5 \times 10^{-3}$	0.0	0.58

$Q_G$  : flow rate of air entering the sparging point;  $F_c$  : flow rate of clean air used to dilute the contaminated air stream; M : mass recovered during the time period indicated;  $C_{L0}=50.94g/m^3$ ; Amount of toluene recovered : 96.26% of that added.

**Table 6.4** Integrated Air Sparging/Biofiltration Process. Conditions for Case Study III

time (min)	$Q_G$ ( $m^3 \text{min}^{-1}$ )	$F_d$ ( $m^3 \text{min}^{-1}$ )	M (g)
69.17	$4.0 \times 10^{-4}$	$2.1 \times 10^{-3}$	0.11
86.37	$6.0 \times 10^{-4}$	$1.9 \times 10^{-3}$	0.03
113.57	$8.0 \times 10^{-4}$	$1.7 \times 10^{-3}$	0.04
197.37	$1.5 \times 10^{-3}$	$1.0 \times 10^{-3}$	0.16
294.48	$2.5 \times 10^{-3}$	$5.0 \times 10^{-4}$	0.45

$Q_G$  : flow rate of air entering the sparging point;  $F_c$  : flow rate of clean air used to dilute the contaminated air stream; M : mass recovered during the time period indicated;  $C_{L_0} = 25.47 \text{g/m}^3$ ; Amount of toluene recovered : 92.65% of that added.

Tables 6.2-6.4 show the flow rate of the air used in sparging the groundwater ( $Q_G$ ), the flow rate of the humidified air used in diluting the air coming out the tank ( $F_d$ ), the duration (time) of the experiment under a given set of  $Q_G$  and  $F_d$  values, and the mass (M) of toluene recovered during each period of the experiment.

Each one of the case studies started by placing 34L of water in the tank and dissolving in it an amount of toluene calculated from the following considerations.

$$Q_G C_G = F C_{Ti} \quad (6.1)$$

where  $F = 2.5 \times 10^{-3} \text{m}^3 \text{min}^{-1}$  and  $C_{Ti} = 1 \text{gm}^{-3}$  as discussed in section 6.1 above.

The initial value of  $Q_G$  was arbitrarily selected, but could neither exceed the value of  $F$  nor be less than  $2 \times 10^{-4} \text{m}^3 \text{min}^{-1}$  which was the minimum flow rate that could be regulated with the equipment in hand.

It was assumed that, initially, toluene (dissolved in the water the night before the experiment was to be carried out) was in equilibrium distribution between the water and

head space of the tank. Hence, it was assumed [equations (6.1) and (4.2)] that

$$0.25Q_G C_{L_0} = 2.5 \times 10^{-3} \text{ g min}^{-1} \quad (6.2)$$

where  $C_{L_0}$  is the initial toluene concentration in the groundwater, and a value of  $m = 0.25$  for the dimensionless Henry constant is used (17).

Once the original  $Q_G$  value for each case study was selected, the amount of toluene ( $M_T$ ) to be added to the vessel was calculated as

$$M_T = V_L C_{L_0} + V_G C_G = (V_L + 0.25V_G) C_{L_0} \quad (6.3)$$

where  $V_L$  and  $V_G$  are the volumes of water (34L) and the head space (28L), respectively, in the tank. The value of  $C_{L_0}$  is given in the footnotes of Tables 6.2-6.4. In the same tables, the amount of toluene recovered during each phase of the sparging process was calculated through numerical integration of the toluene concentration profile at the exit of the tank.

As can be seen from Tables 6.2-6.4 in each case study, the experiment started with a low  $Q_G$  value and high  $F_d$  value while the sum  $Q_G + F_d$  was always kept constant at the  $F$  value of  $2.5 \times 10^{-3} \text{ m}^3 \text{ min}^{-1}$  (see section 6.1). Progressively, the value of  $Q_G$  was increased till it reached the  $F$  value while the value  $F_d$  decreased till it became zero, implying that in the last sparging period all air was directed through the tank.

The intent of varying the relatively ratio of  $Q_G$  to  $F_d$  was to maintain a relatively constant toluene concentration at the entrance of the biofilter. In addition, the intent was for the toluene concentration never to exceed the value of  $1 \text{ gm}^{-3}$  (see section 6.1). These objectives were more or less met, as can be judged from curves 1 in Figures 6.1(a), 6.2(a) and 6.3(a).



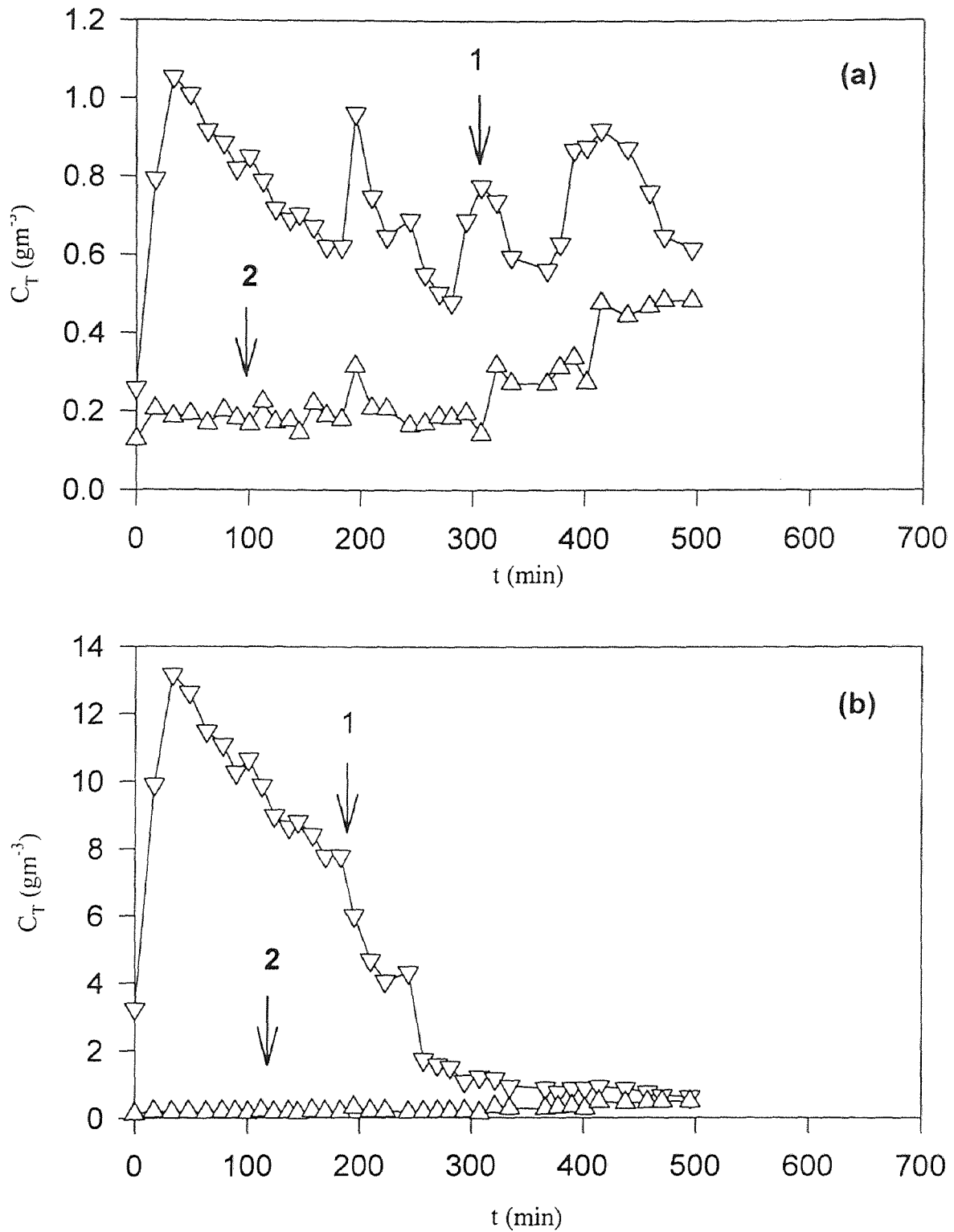


**Figure 6.1** Toluene concentration profiles for Case Study I. (a): at the inlet and outlet of the biofilter unit; curves 1 and 2, respectively. (b): at the exit of the tank and outlet of the biofilter; curves 1 and 2, respectively.

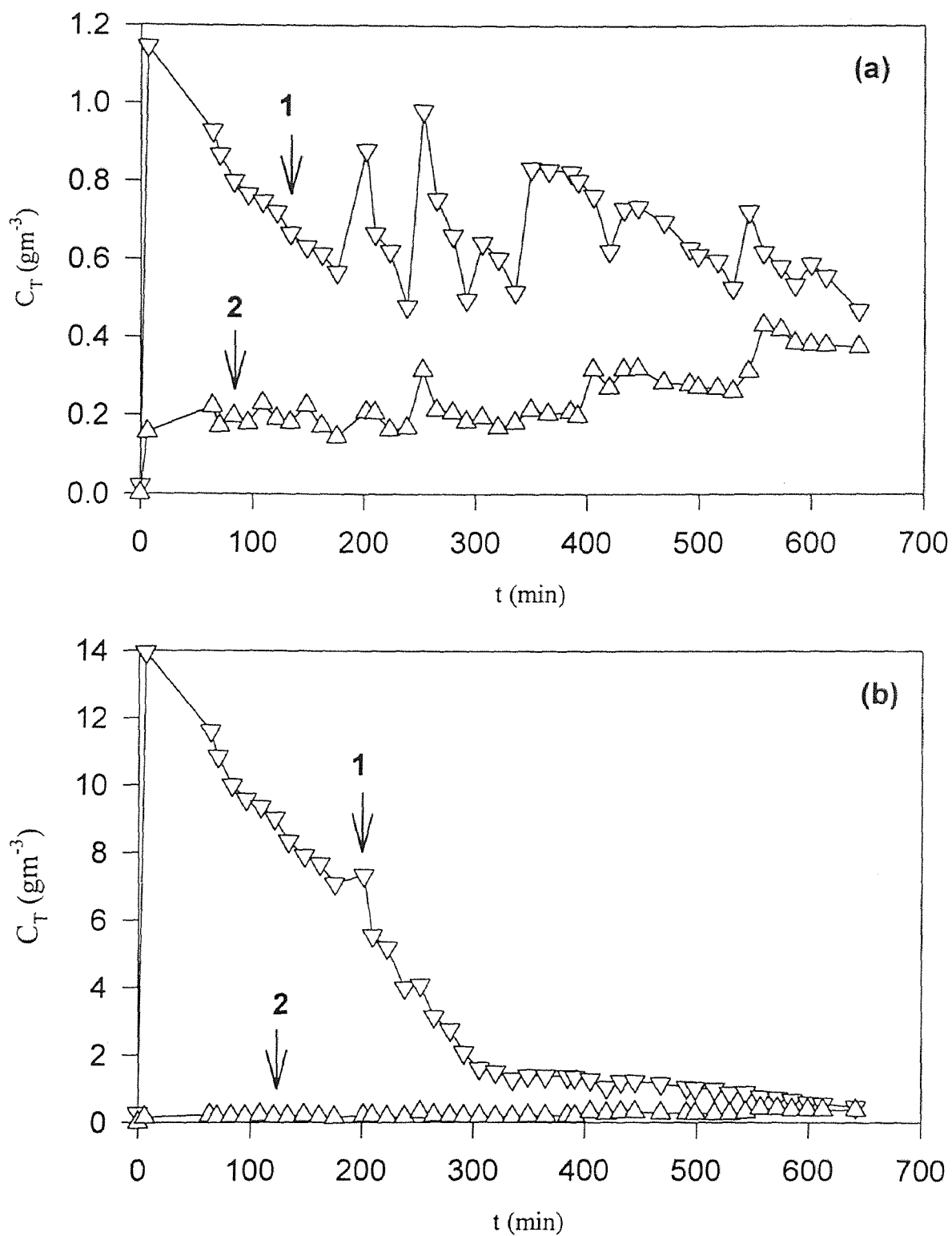


**Figure 6.2** Toluene concentration profiles for Case Study II. (a): at the inlet and outlet of the biofilter unit; curves 1 and 2, respectively. (b): at the exit of the tank and outlet of the biofilter; curves 1 and 2, respectively.

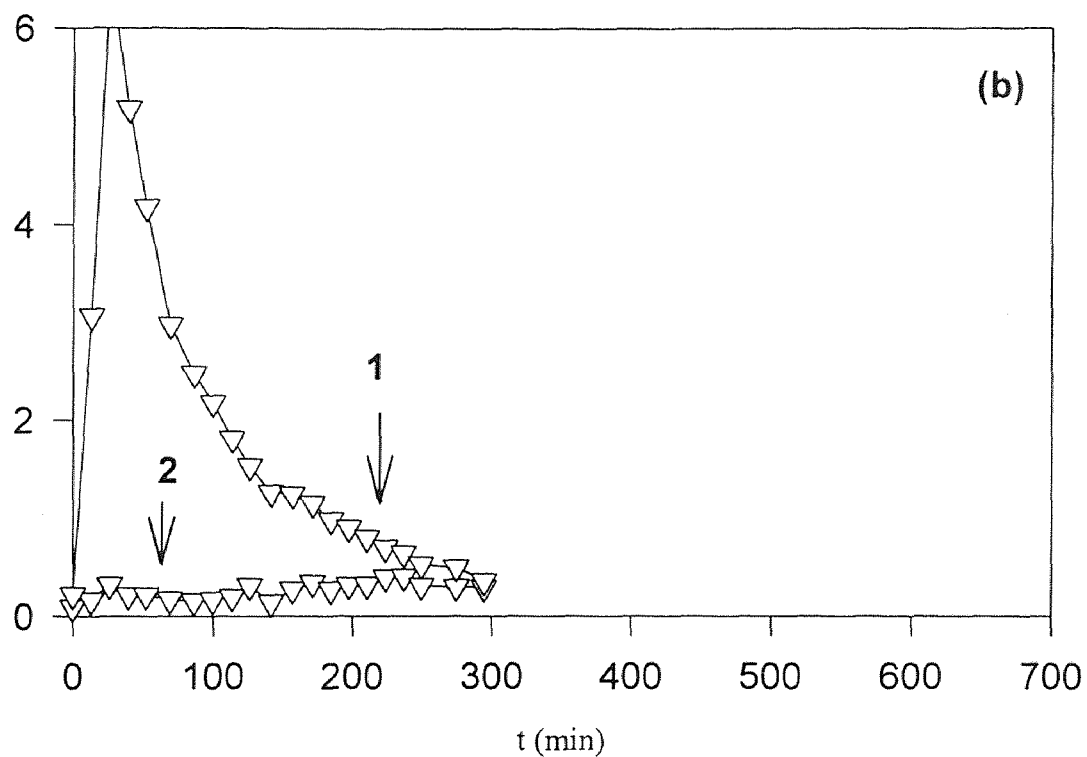
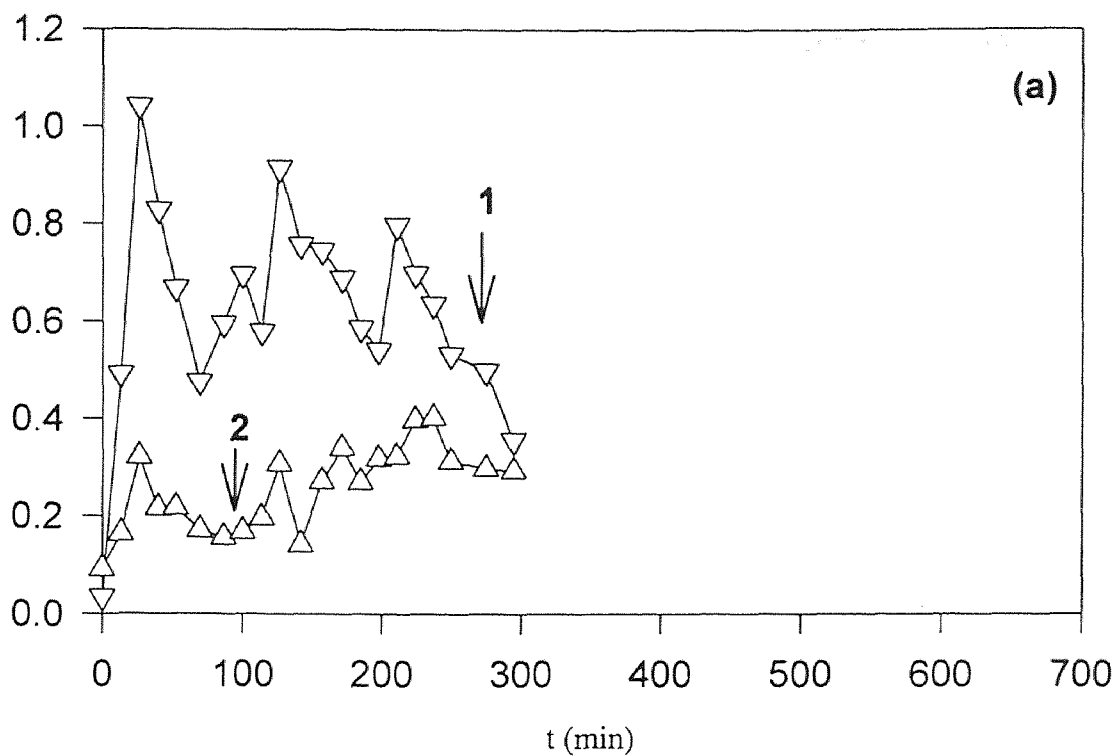


**Figure 6.3** Toluene concentration profiles for Case Study III. (a): at the inlet and outlet of the biofilter unit; curves 1 and 2, respectively. (b): at the exit of the tank and outlet of the biofilter; curves 1 and 2, respectively.

The second, and probably the key, objective of these experiments was to show that toluene concentrations at the exit of the biofilter never exceed ASIL limits. This was not achieved as can be judged from curves 2 in Figures 6.1-6.3. In Case Study I (Figure 6.1) the objective was met during the first 300 min of the experiment with one exception at 200min. In Case Study II (Figure 6.2) the objective was met during the first 400min with, again, one exception at about 250min. For Case Study III (Figure 6.3) one could say that for all practical purposes the objective was never met.

From curves 2 in Figures 6.1 and 6.2 it is interesting to observe that although the inlet concentrations of toluene (curves 1) vary during the first 300 and 400min, respectively, the concentrations at the exit of the biofilter are essentially constant. One could possibly argue that during the initial periods, although the toluene concentration at the inlet of the biofilter drops over most of the time, the internal concentrations (in the filter bed) remain constant as desorption phenomena occur as discussed by Androusofoulou (1), Sharefdeen (17) and others. The behavior towards the end of the process, when ASIL levels are not met, are hard to explain. In fact, this behavior seems to contradict the findings of Stamatiadis (19) who, through modeling, showed that during transients exit concentrations do not exceed the steady state values calculated based on the maximum inlet toluene concentration. In the cases considered here, and based on the finding from steady state experiments (Table 6.1) the exit concentrations from the biofilter should never exceed  $0.26\text{gm}^{-3}$ , since  $\tau = 6.6\text{min}$  and  $C_{Ti}$  essentially never exceeds  $1\text{gm}^{-3}$ . The only potential explanations are the following. First, the adsorption characteristics were not properly modeled and thus, the work of Stamatiadis (19) is based on an incorrect model. The second, and the most probable, is that towards the end of the

process and as more air is passed through the groundwater tank, contacting time is low for completely humidifying the air stream. Thus, a partially humidified airstream is supplied to the biofilter, the packing is partially dried, and the performance deteriorates.

Another interesting observation is that, albeit over short periods of time, the concentrations exiting the tank immediately after initiation of Case Study II are higher than those predicted by thermodynamic equilibrium distribution. This could be only explained by incomplete mixing of toluene with water. Possibly a layer of toluene was sitting on the water surface and got quickly volatilized once air started passing through the tank.

### **6.3 Distribution of Toluene Between Water and Sparged Air**

Experiments were performed with the apparatus shown in Figure 5.2. Some experiments employed a 2.2L flask carrying the toluene solution while others employed a 1.1L flask. Since in all cases the volume of the aqueous solution was 1L, use of a different flask implied a different volume ratio of the head space ( $V_G$ ) and liquid ( $V_L$ ). The experiments performed can be classified primarily into two categories. The first, involved experiments in which the same amount of toluene was added to the flask whereas the volumetric flow rate of the sparging air ( $Q_G$ ) was varied between experiments. The second category, involved experiments with the same  $Q_G$ , but the amount of toluene added to the flask varied between experiments. The experimental data were analyzed by using equation (4.10) and led to the calculation of the value of  $\sigma$  [via equation (4.13)].

Results are shown in Tables 6.5-6.7 and, in graphical form, Figures 6.4 and A-1 to A-10 of Appendix A. In graphs (a) of the foregoing figures the regressed line [to equation

(4.10)] is shown, while in graphs (b) the curves represent equation (4.9) using the values of constants from the regression.

**Table 6.5** Data from toluene distribution experiments when  $V_G = 1.2L$ . In all experiments an amount of 8.66mg toluene was added to 1L water.

Experiment	$Q_G$ ( $m^3 \text{ min}^{-1}$ )	$\sigma$	$C_{Lo}$ ( $gm^{-3}$ )	$R^2$
E-1	$1.0 \times 10^{-4}$	0.71	5.874	0.996
E-2	$2.0 \times 10^{-4}$	0.69	5.111	0.988
E-3	$3.0 \times 10^{-4}$	0.46	4.984	0.981
E-4	$4.0 \times 10^{-4}$	0.37	4.485	0.989
E-5	$5.0 \times 10^{-4}$	0.28	4.916	0.966
E-6	$6.0 \times 10^{-4}$	0.32	4.921	0.983

**Table 6.6** Data from toluene distribution experiments when  $V_G = 0.1L$ . In all experiments an amount of 8.66mg toluene was added to 1L water.

Experiment	$Q_G$ ( $m^3 \text{ min}^{-1}$ )	$\sigma$	$C_{Lo}$ ( $gm^{-3}$ )	$R^2$
E-7	$1.0 \times 10^{-4}$	0.45	5.326	0.987
E-8	$2.0 \times 10^{-4}$	0.29	5.863	0.994
E-9	$3.0 \times 10^{-4}$	0.30	6.839	0.991

**Table 6.7** Data from toluene distribution experiments when  $V_G = 0.1L$  and  $Q_G = 1.0 \times 10^{-4} m^3 \text{ min}^{-1}$ . Amount of toluene added varies.

Experiment	Toluene added(g)	$\sigma$	$C_{Lo}$ ( $gm^{-3}$ )	$R^2$
E-10	0.00103	0.32	1.019	0.977
E-11	0.00433	0.35	2.738	0.991
E-7	0.00866	0.45	5.326	0.987

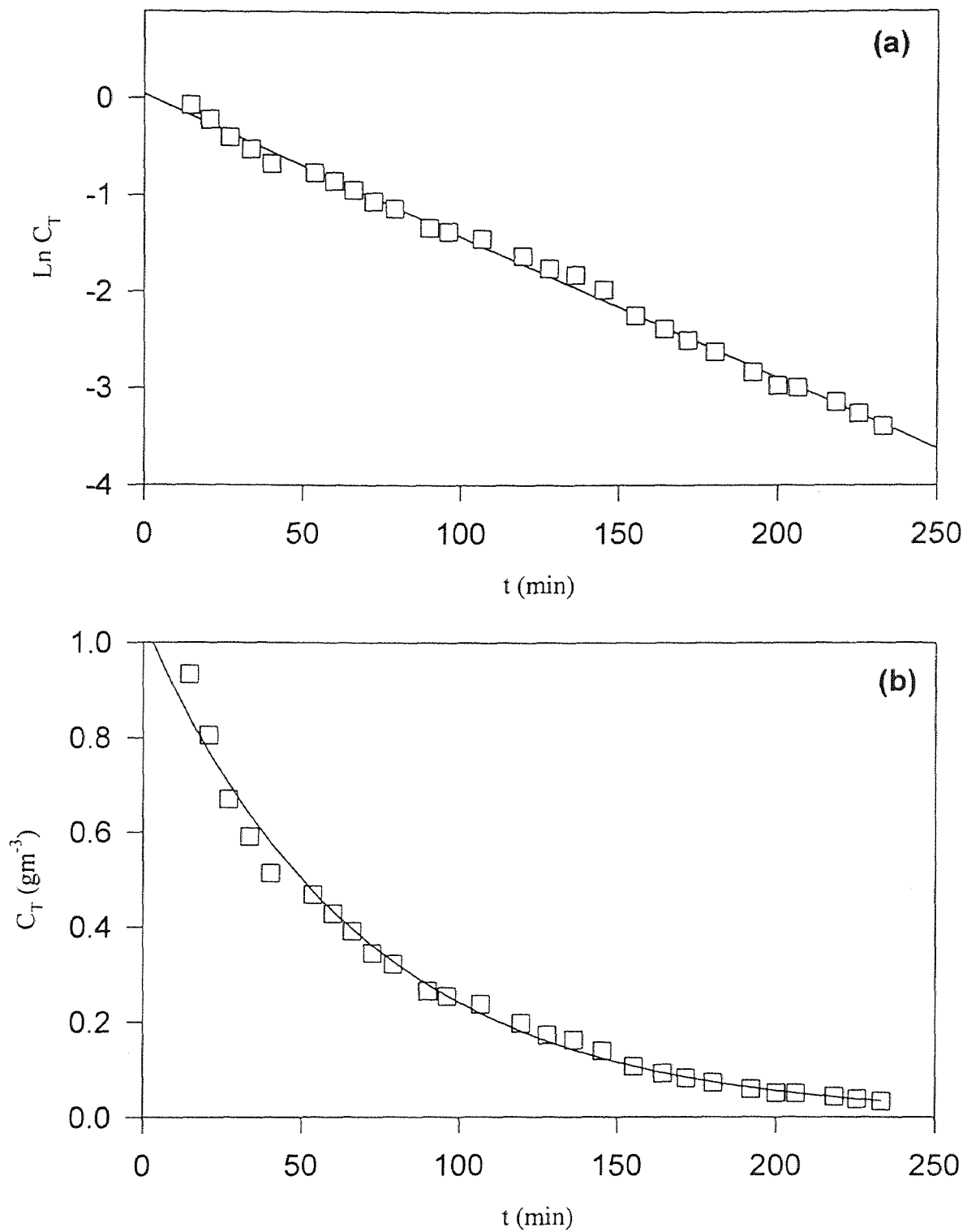


**Figure 6.4** Toluene concentration data for experiment E-1 in (a): semilogarithmic and (b): arithmetic scale. Lines and curves represent regressions.

From Tables 6.5 and 6.6 one can see that the trend is for  $\sigma$  to decrease with increasing  $Q_G$  values. It is also worth observing that  $\sigma$  never comes close to 1, which would indicate thermodynamic equilibrium. From the correlation coefficient ( $R^2$ ) one can see that the fitting of the data to equation (4.10) is not very satisfactory. It must be also mentioned that the initial data from each run had to be omitted for getting the fitting shown. This also explains the variation of  $C_{L0}$  values among experiments E-1 to E-6 and E-7 to E-9. For these two groups of experiments one would expect a constant  $C_{L0}$  value since the flasks were charged with the same amount of water and toluene. This apparent inconsistency can be explained by using the arguments presented at the end of Chapter 4.

Comparing the results from the following three pairs of experiments: E-1 and E-7, E-2 and E-8, E-3 and E-9 one can see that a smaller value is obtained for  $\sigma$  when the  $V_G/V_L$  ratio decreases. Due to the geometry of the flasks, one could argue that the same  $Q_G$  leads to worse sparging (less area for mass transfer) of the liquid in the smaller flask. This is a clear indication that  $\sigma$  masks mass transfer effects.

From Table 6.7 one can see that when  $V_G$  and  $Q_G$  are constant, the value of  $\sigma$  increases as the amount of toluene added increases. An increased amount of toluene added to the same amount of water leads to higher concentrations and thus, a higher driving force for the mass transfer which may explain the observed results.

The apparatus shown in Figure 5.2 was also used in an experiment during which the value of  $Q_G$  was varied. Essentially, the experiment had three phases each one of which lasted for 1 hour. The results are shown in Table 6.8. Data from each phase were regressed to equation (4.10) and are shown in Figures A-11, A-12 and A-13 of



**Table 6.8** Toluene distribution from an experiment with varying  $Q_G$ . Toluene added: 8.6mg;  $V_G=0.1L$

Experiment	$Q_G$ ( $m^3 min^{-1}$ )	$\sigma$	$C_{Lo}(gm^{-3})$	$R^2$
B-12a	$1.0 \times 10^{-4}$	0.56	5.584	0.961
B-12b	$2.0 \times 10^{-4}$	0.48	2.485	0.981
B-12c	$3.0 \times 10^{-4}$	0.35	0.637	0.975

Appendix A. The complete profile (made of three (b) segments of Figures A-11 to A-13) is shown in Figure 6.5. Although the regressed curve seems to adequately represent the data, the results are confusing. The first phase of this experiment (i.e., experiment E-12a) is identical to experiment E-7. Yet, the values of  $\sigma$  and  $C_{Lo}$  are significantly different. Furthermore, the second phase of the experiment (experiment E-12b) resembles experiment E-8 except for the fact that experiment E-8 started with more toluene. The same can be said for the third phase (experiment E-12c) and experiment E-9. Comparing the values of  $\sigma$  for the pairs E-8 and E-12b; E-9 and E-12c one can see that  $\sigma$  increases as the amount of toluene present at the start-up of the experiment decreases. This is exactly opposite to what was observed in the experiments reported in Table 6.7.

An experiment similar to E-12 was performed by using the tank employed in the integrated air sparging/biofiltration experiments. The vessel was charged with 34L of water and 1.73g toluene. The volume of the head space was 28L. The rate of air sparging was increased over time. The experiment had five phases of different duration. Results from each phase are shown in Table 6.9 and Figures B-1 through B-5 of Appendix B. The complete profile is shown in Figure 6.6. The results were disappointing as values of  $\sigma$

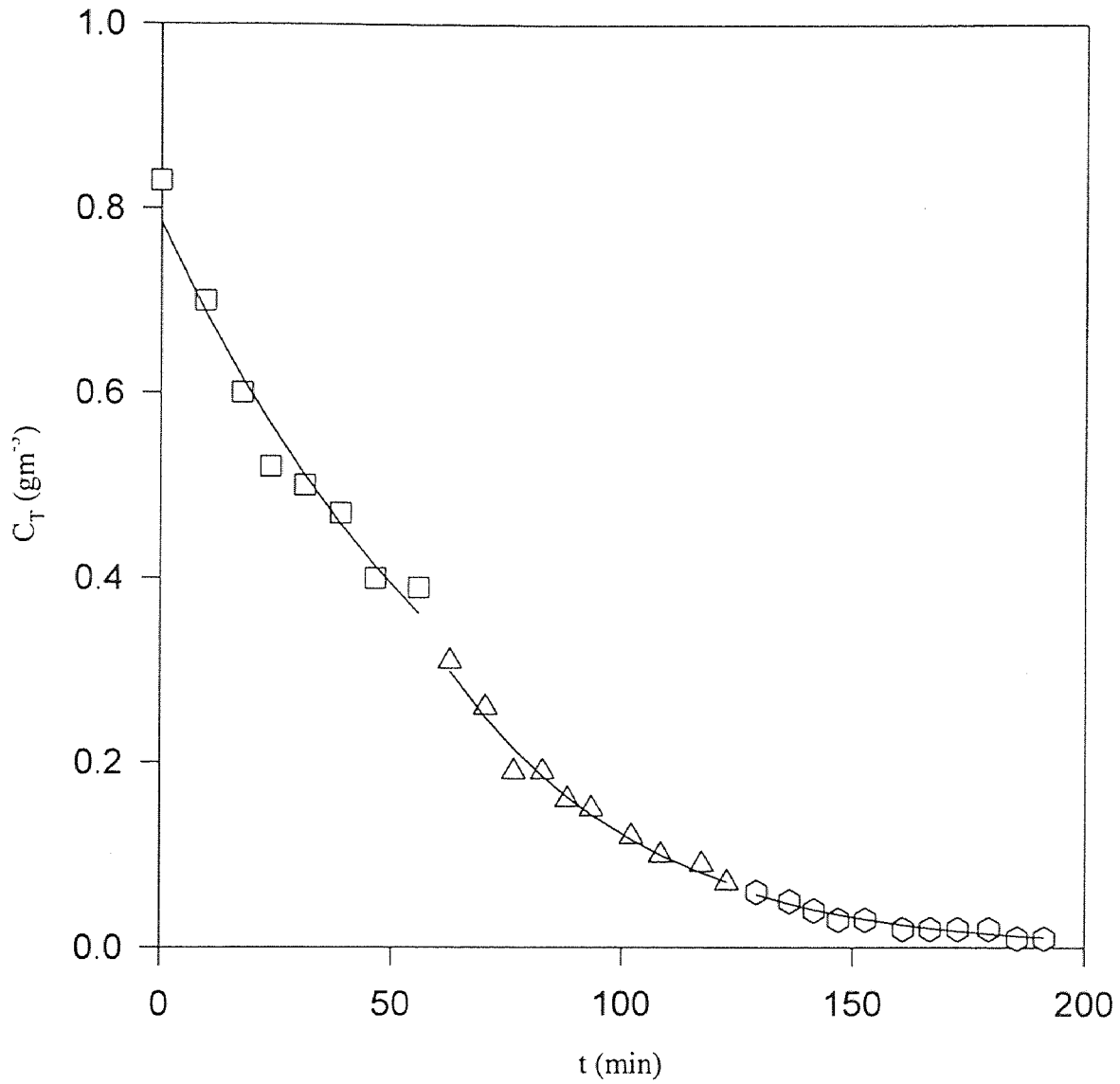


**Figure 6.5** Toluene concentration profile as a function of time for the three phases of experiment E-12

higher than 1 were obtained, correlations ( $R^2$ ) were poor, and in some cases (phase 2) the  $C_{L0}$  values were unrealistic. Also, the trend in  $C_{L0}$  values does not make sense in most cases. It is likely that an amount of undissolved toluene was present on the surface of the water.

**Table 6.9** Data from a toluene distribution experiment with varying  $Q_G$ . Toluene added: 1.73g;  $V_G = 28L$ ;  $V_L = 34L$ .

Figure	$Q_G$ ( $m^3 min^{-1}$ )	$\sigma$	$C_{L0}$ ( $gm^{-3}$ )	$R^2$	Duration (min)
B-1	$2.0 \times 10^{-4}$	5.03	11.679	0.975	182
B-2	$4.0 \times 10^{-4}$	50.24	0.047	0.982	61
B-3	$8.0 \times 10^{-4}$	1.26	5.455	0.982	24
B-4	$1.6 \times 10^{-4}$	0.25	16.913	0.968	83
B-5	$2.5 \times 10^{-4}$	0.32	13.473	0.931	131

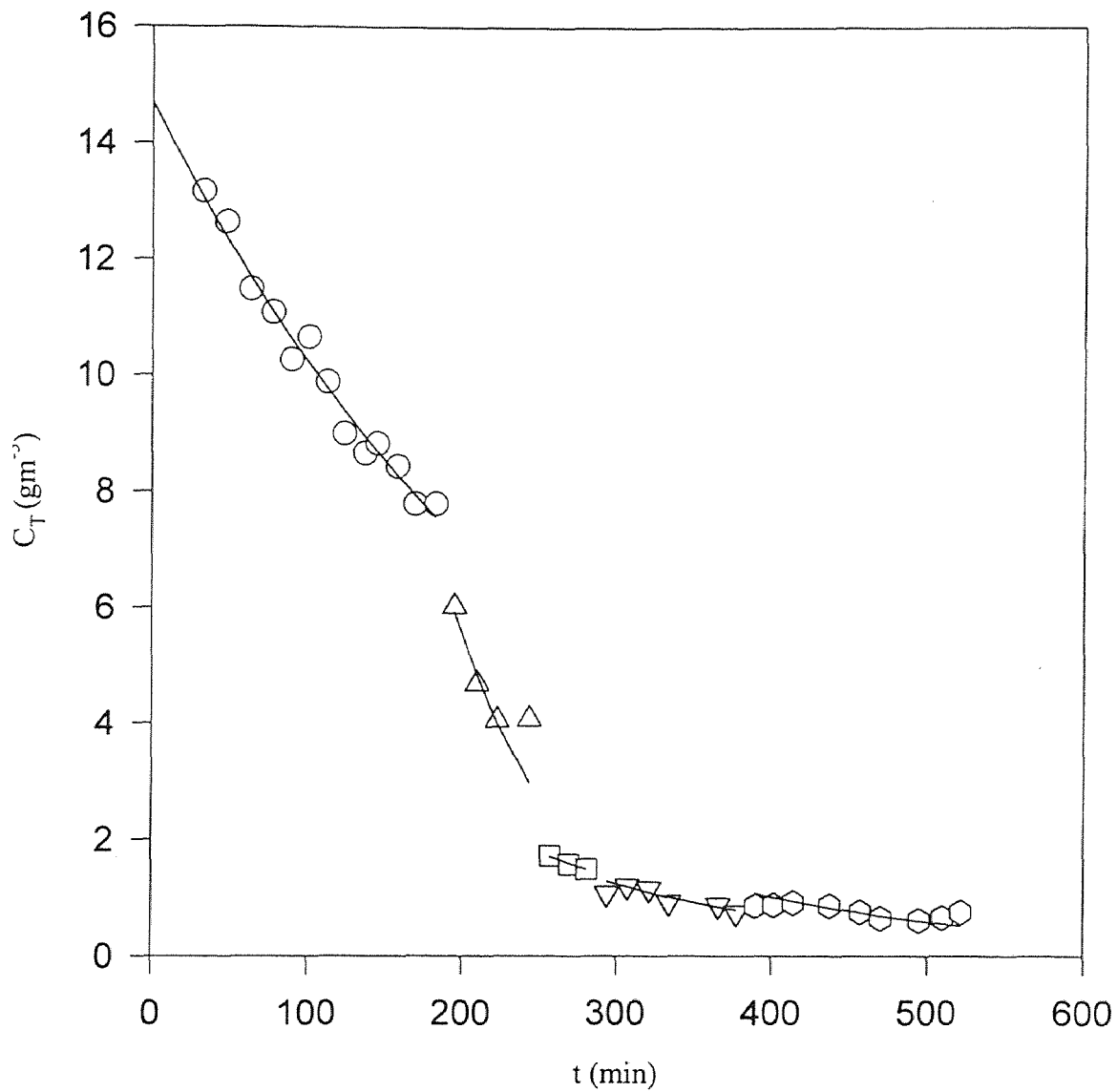


**Figure 6.6** Toluene concentration profile as a function of time for the five phases of experiment B.

## CHAPTER 7

### CONCLUSIONS AND RECOMMENDATIONS

The results of this study have shown through experiments that an integrated air sparging/biofiltration process is feasible. However, there was much less success with efforts to experimentally show that the process can always work under desired conditions.

It was possible to show that over a significant amount of time the concentrations at the exit of the biofilter are constant despite the fluctuations at the inlet conditions. This has been achieved through an extensive trial and error approach regarding the flowrate of the air sparged into the contaminated water and its subsequent dilution with clean, humidified, air. It was not possible to actually predict the flowrates required for the desired outcome. When concentrations at the exit of the biofilter were constant, they were at levels satisfying the ASIL requirements of regulations. However, in all cases tried, it was observed that after a few hours and when essentially all air was directed into the contaminated water (i.e., no dilution) the concentration of the model compound used (toluene) at the outlet of the biofilter increased and, for the most part, did not meet the ASIL requirements. This failure can be attributed to moisture effects. The air was not completely humidified and this caused the packing material to dry and effectiveness of biofiltration to decrease. Future experiments should focus more on moisture control in the biofilter. These results suggest that the air coming out of groundwater should be passed through a humidification tower before it enters the biofilter. This can possibly create

problems with relatively highly water soluble compounds as a fraction of the contaminant may be transferred to the water leading to a need for its treatment.

The efforts made in predicting the distribution of toluene between the water and the sparged air did not lead to any conclusive results. Hence, the ability to predict the required flowrates for air sparging in order to maintain a relatively smooth biofilter performance is questionable at this point. It is clear that the distribution (essentially mass transfer) is affected by the concentration of the pollutant in the water and the residence time of the air in the water reservoir (aquifer). Efforts to describe these effects using a single parameter, as was done in this thesis, appear to be destined to fail. More detailed models clearly accounting for mass transfer and the area available for it need to be used. It appears, however, that during the course of an integrated air sparging/biofiltration process the mass transfer characteristics change (due to changing flowrates and concentrations). This variability has never been considered and two earlier, theoretical/modeling, studies considered either equilibrium or a constant deviation from it (4, 19). Hence, there is a need for more systematic studies regarding the air sparging part of the integrated process, and this effort should be at both the experimental and modeling levels.

There is no doubt that in actual situations where a contaminant may be present not only in the water, but also sorbed on the soil, the situation will be much more complex. There is a need for adequate simulation of an aquifer within an experimental setting in order to reduce the pilot scale work before process implementation.

Although the motion of an integrated air sparging/biofiltration process may appear simple, this study has shown that there are still many non-well understood issues. These need to be clarified if this process is to have a wide spread application in remediating the many existing contaminated sites.

## APPENDIX A

### TOLUENE CONCENTRATION DATA FOR EXPERIMENTS: E-2 TO E-12



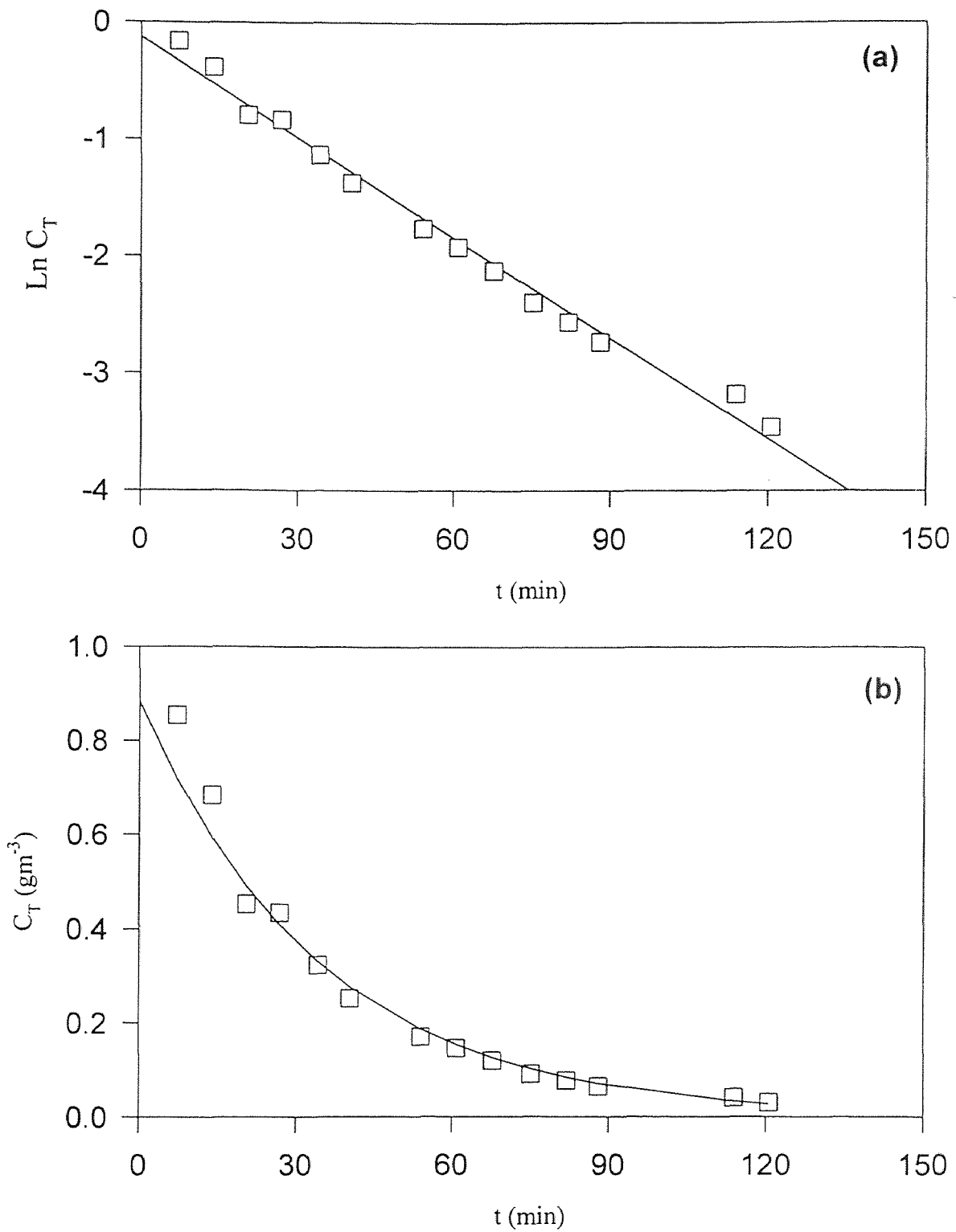


**Figure A-1** Toluene concentration data for experiment E-2 in (a): semilogarithmic and (b): arithmetic scale. Lines and curves represent regressions.

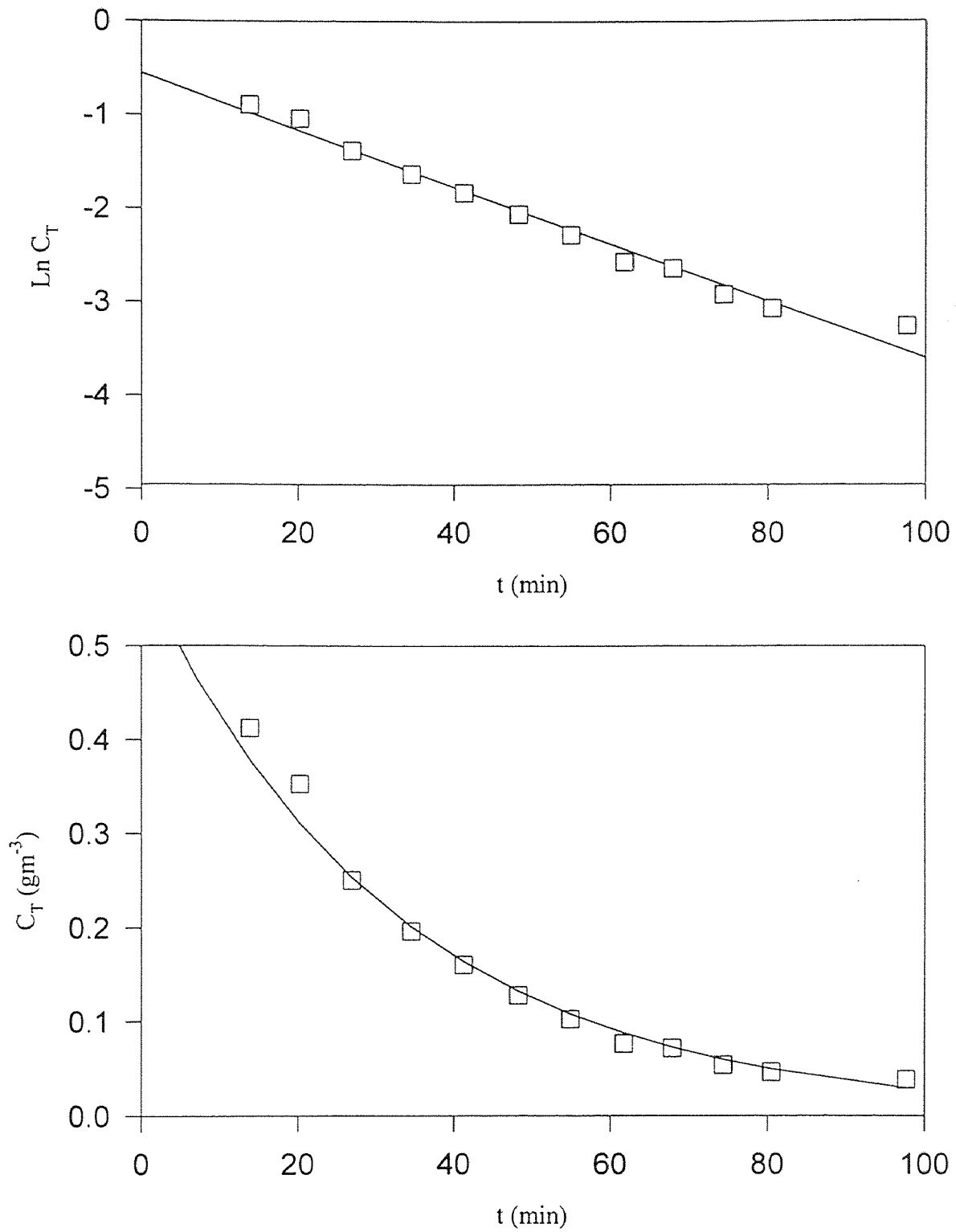


**Figure A-2** Toluene concentration data for experiment E-3 in (a): semilogarithmic and (b): arithmetic scale. Lines and curves represent regressions.

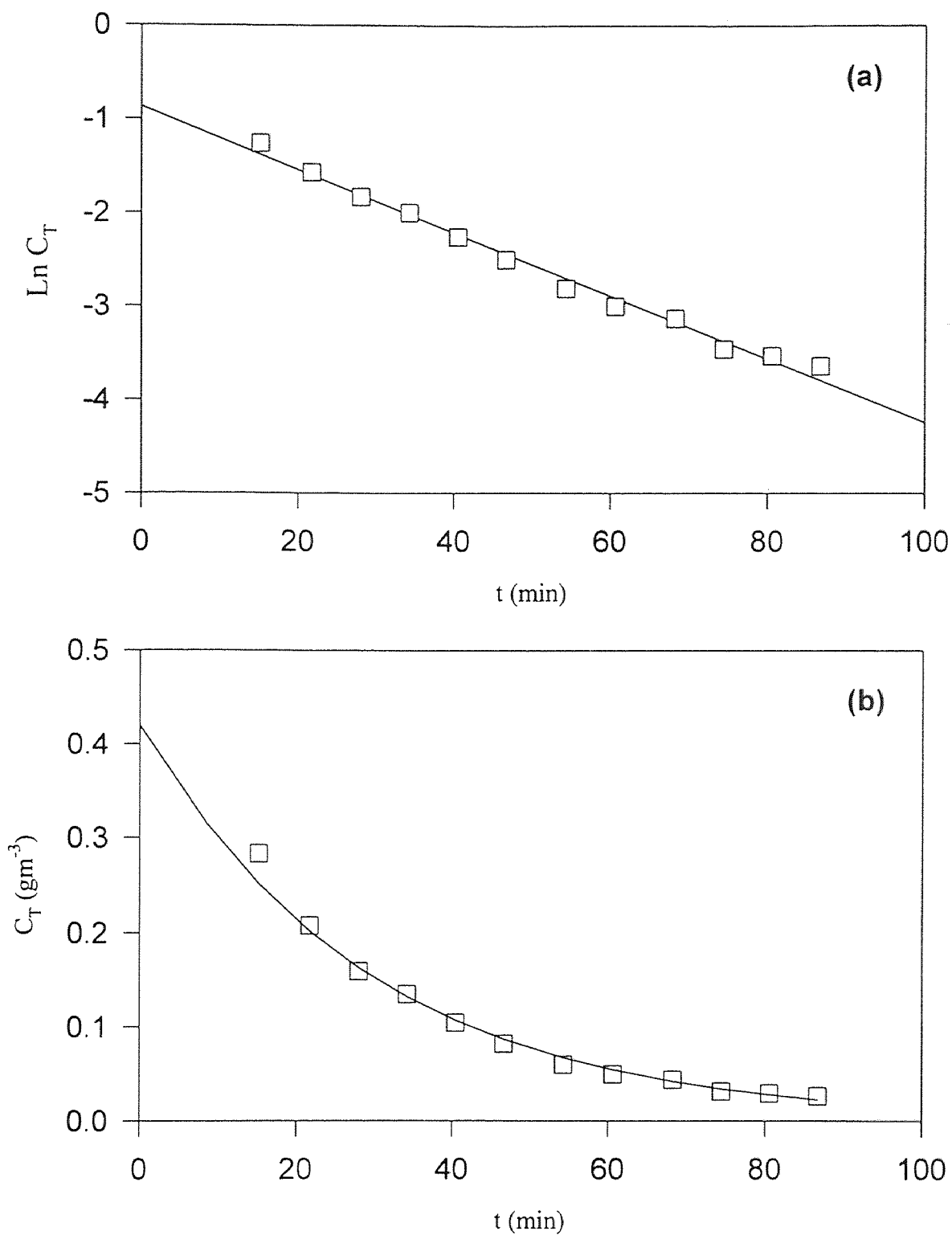


**Figure A-3** Toluene concentration data for experiment E-4 in (a): semilogarithmic and (b): arithmetic scale. Lines and curves represent regressions.

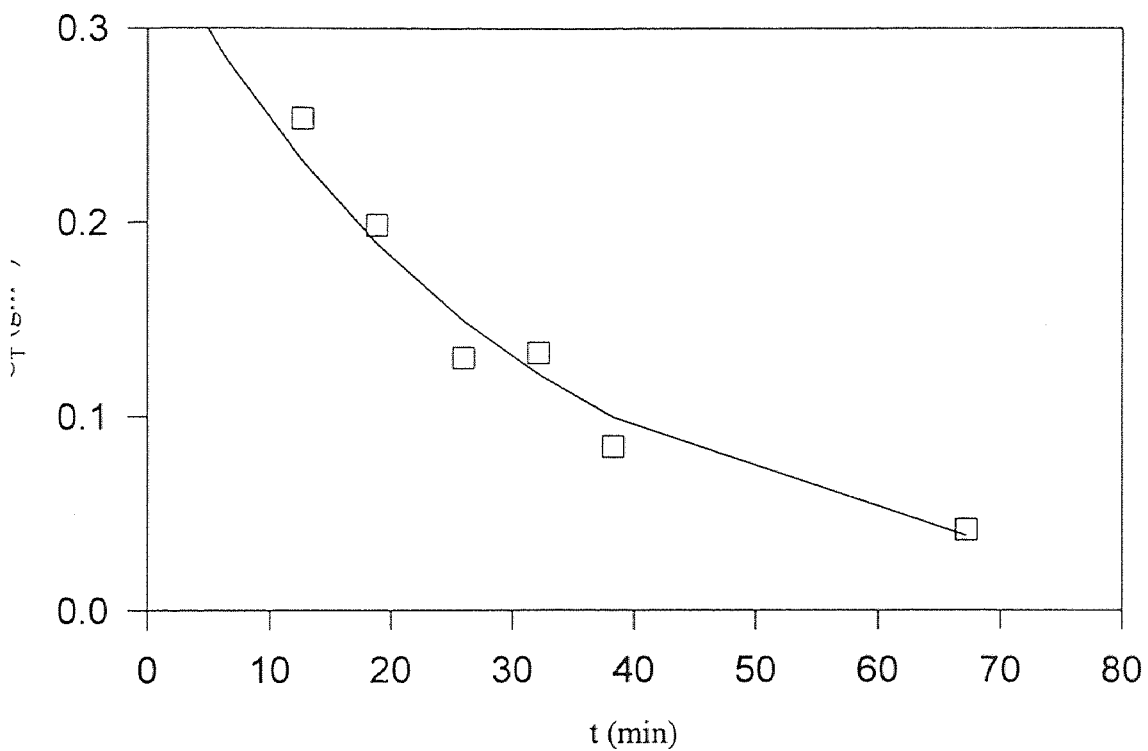
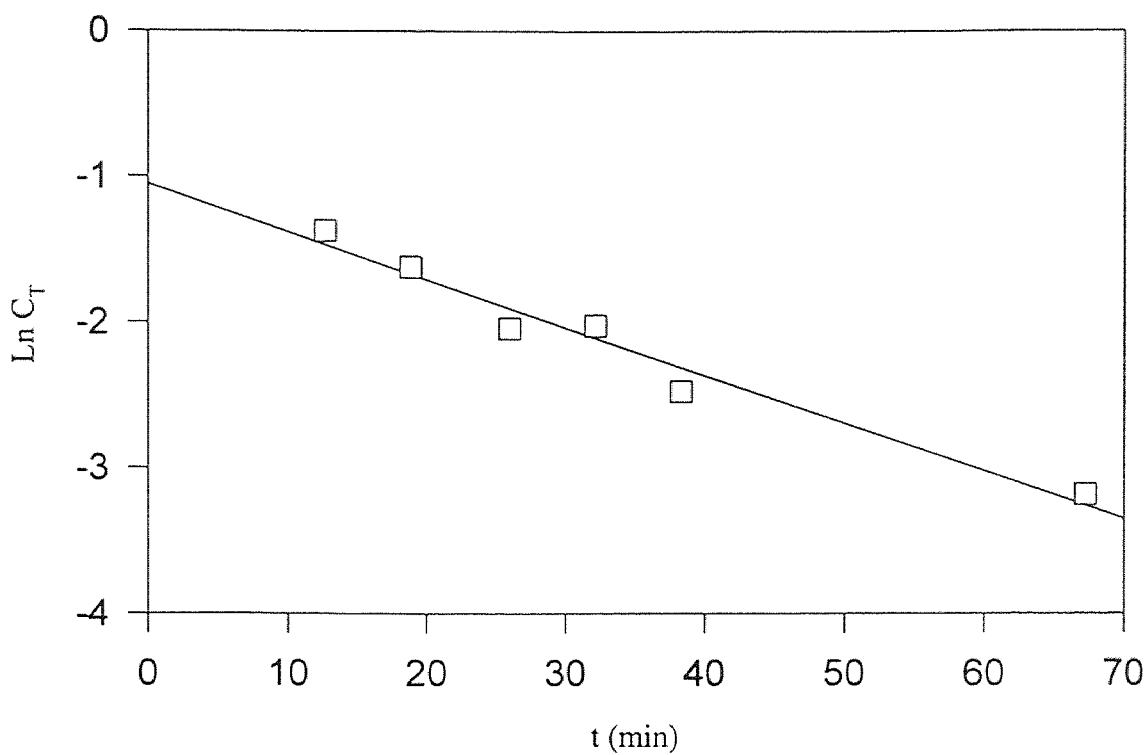


**Figure A-4** Toluene concentration data for experiment E-5 in (a): semilogarithmic and (b): arithmetic scale. Lines and curves represent regressions.

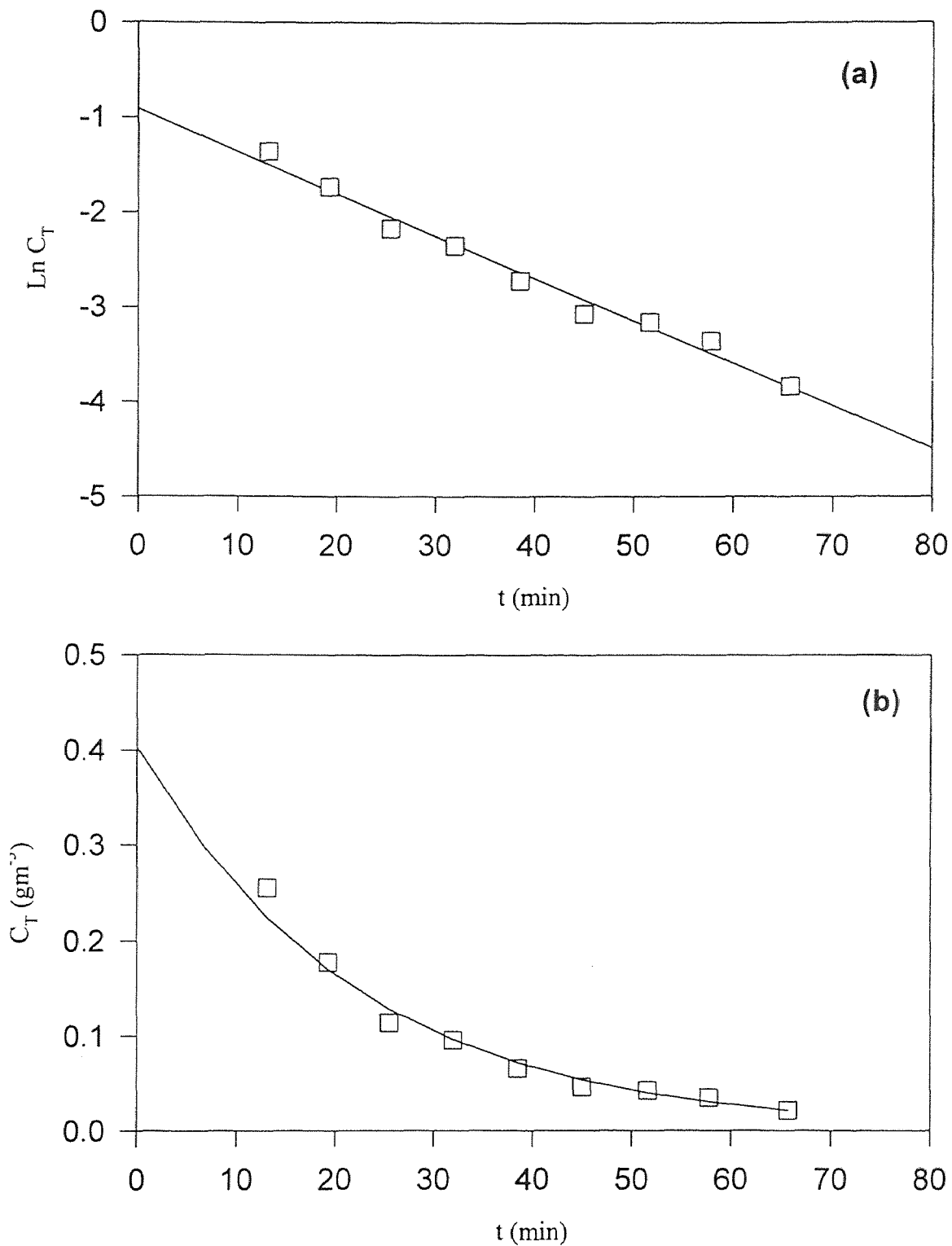


**Figure A-5** Toluene concentration data for experiment E-6 in (a): semilogarithmic and (b): arithmetic scale. Lines and curves represent regressions.

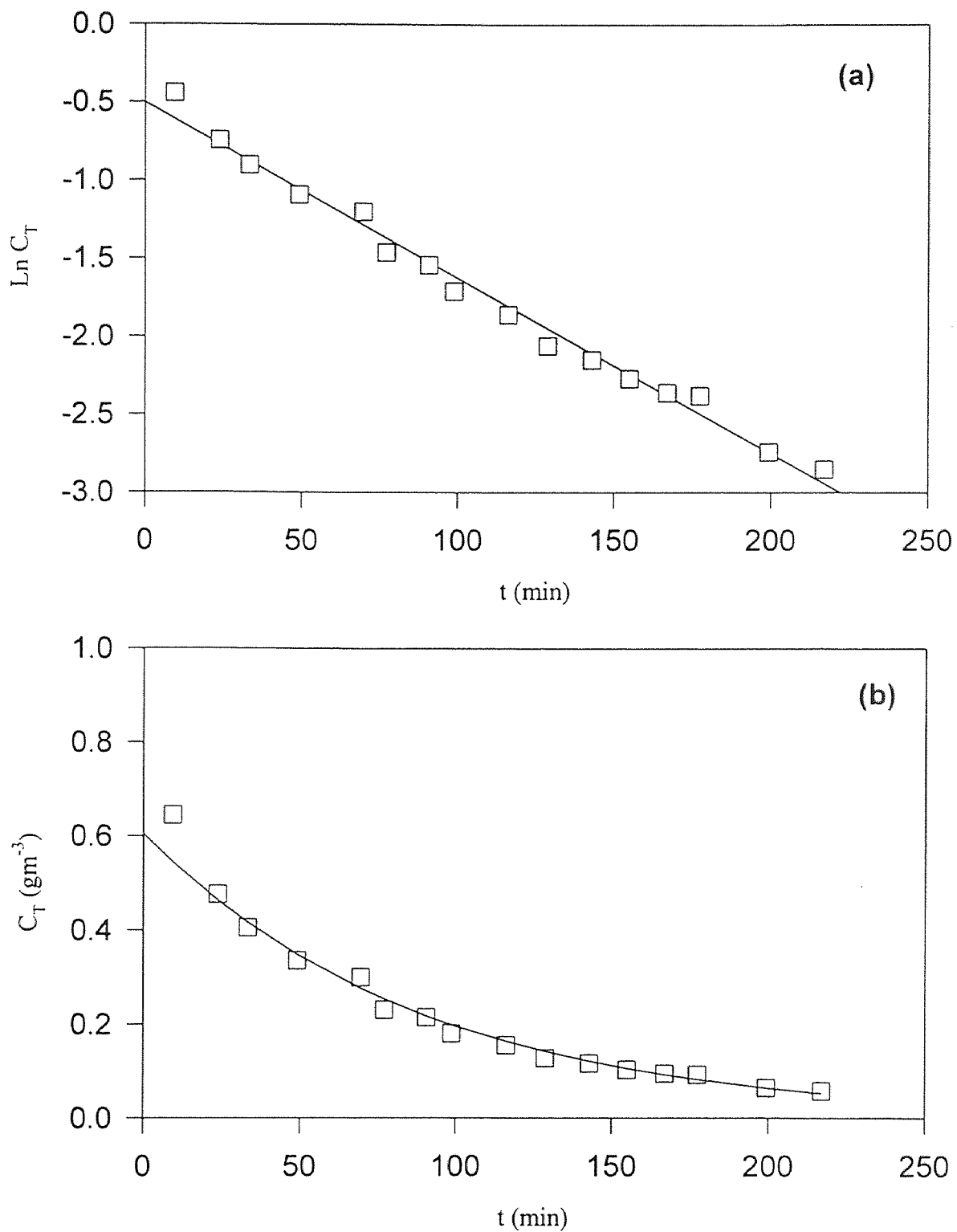


**Figure A-6** Toluene concentration data for experiment E-7 in (a): semilogarithmic and (b): arithmetic scale. Lines and curves represent regressions.

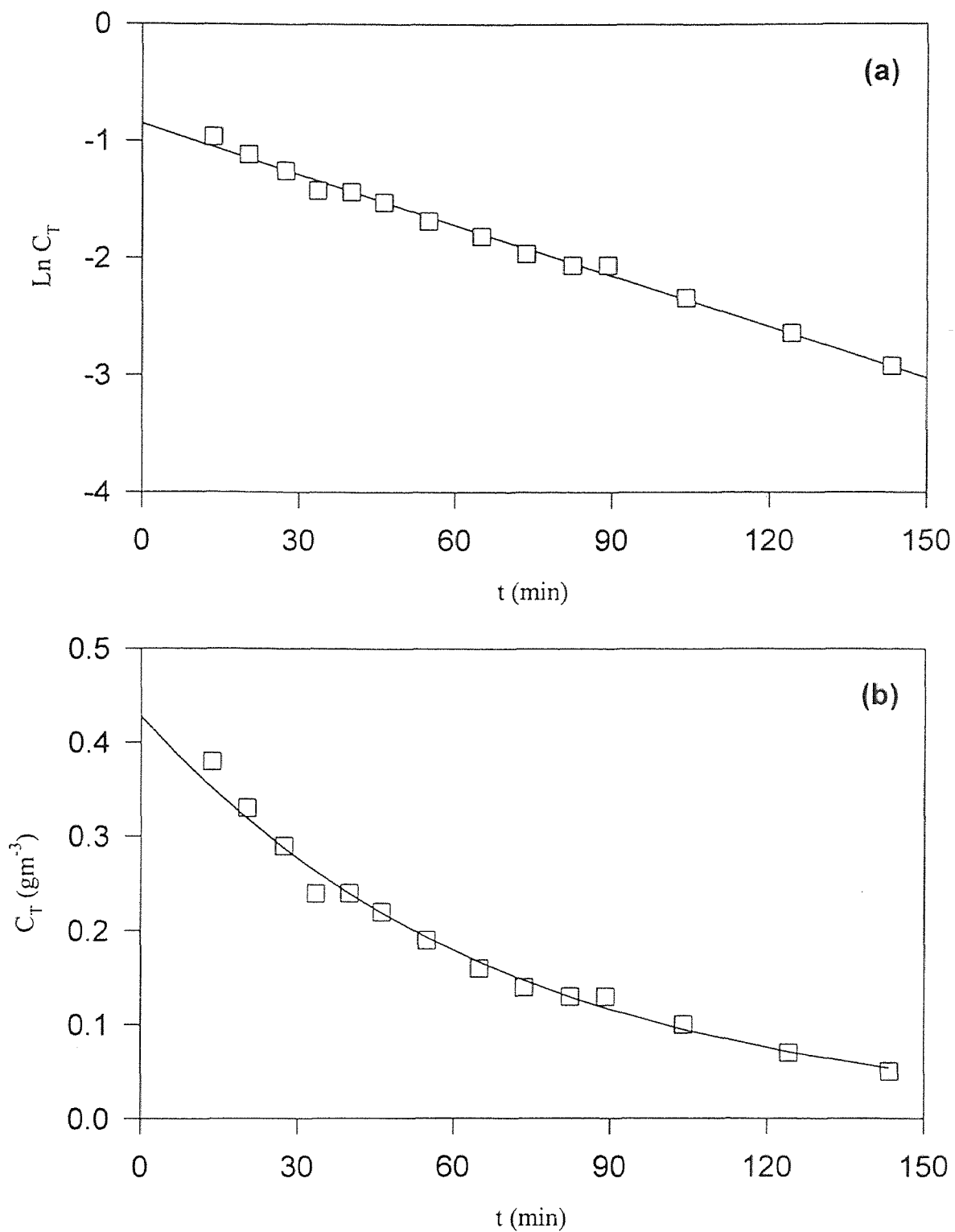


**Figure A-7** Toluene concentration data for experiment E-8 in (a): semilogarithmic and (b): arithmetic scale. Lines and curves represent regressions.

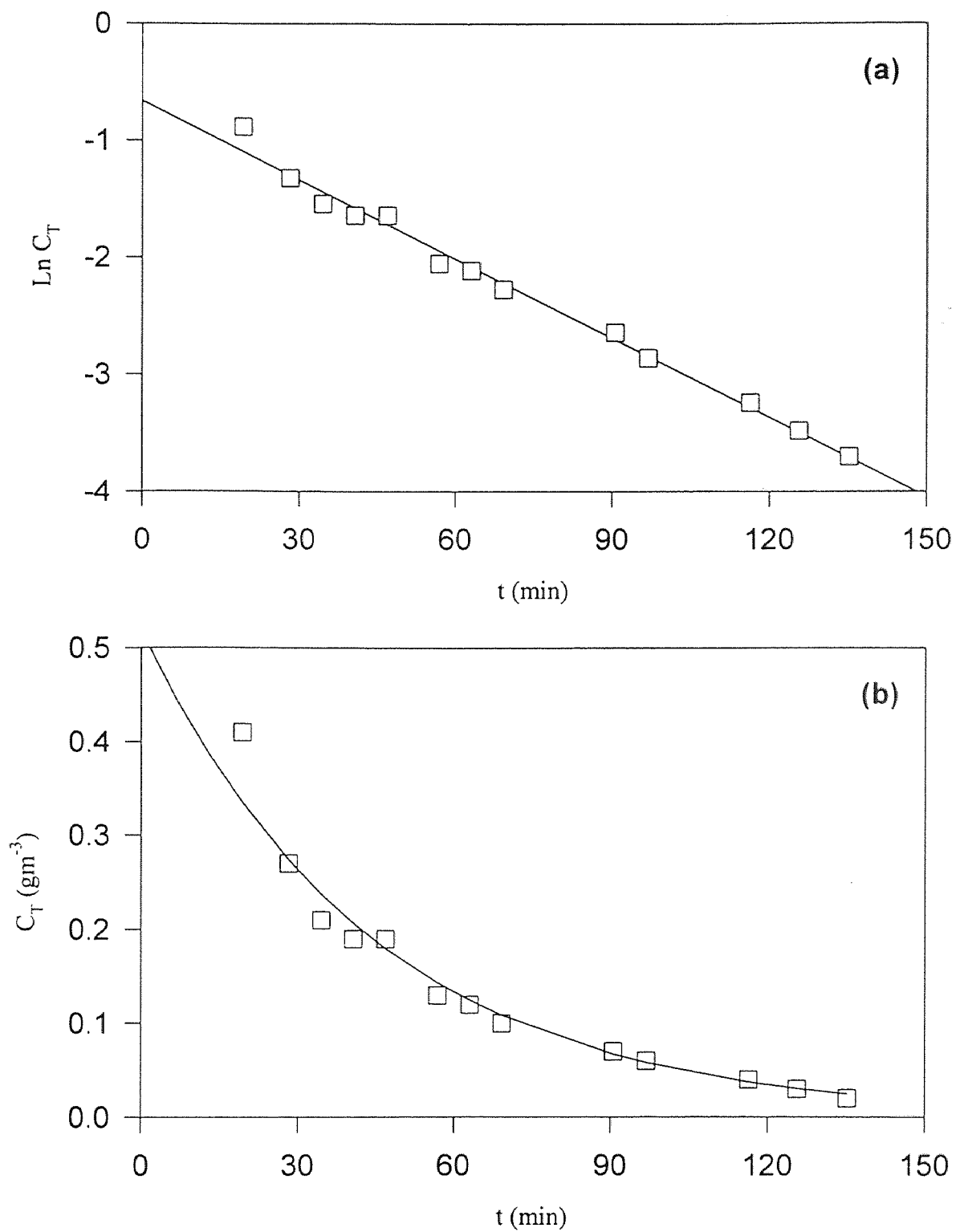


**Figure A-8** Toluene concentration data for experiment E-9 in (a): semilogarithmic and (b): arithmetic scale. Lines and curves represent regressions.



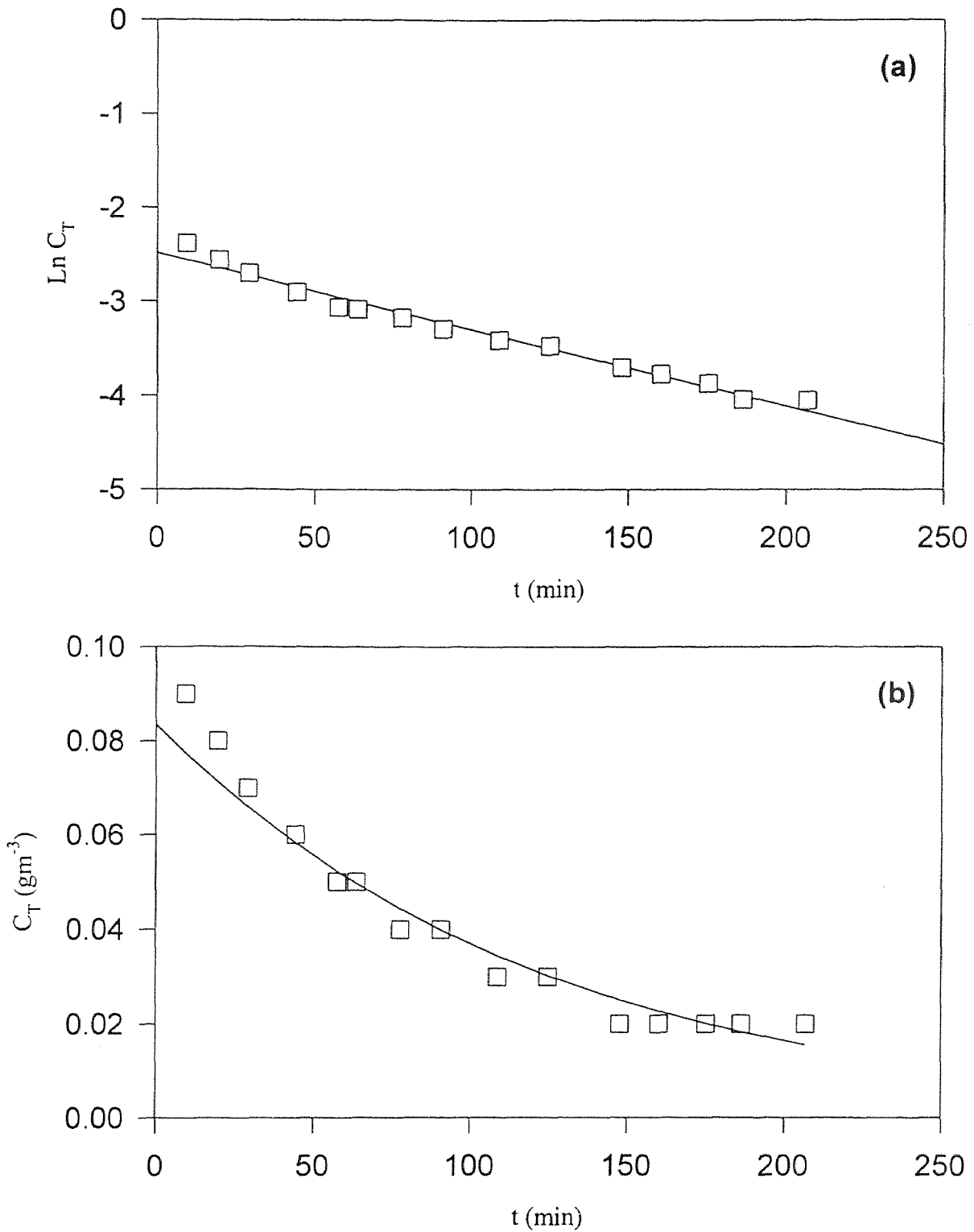


**Figure A-9** Toluene concentration data for experiment E-10 in (a): semilogarithmic and (b): arithmetic scale. Lines and curves represent regressions.

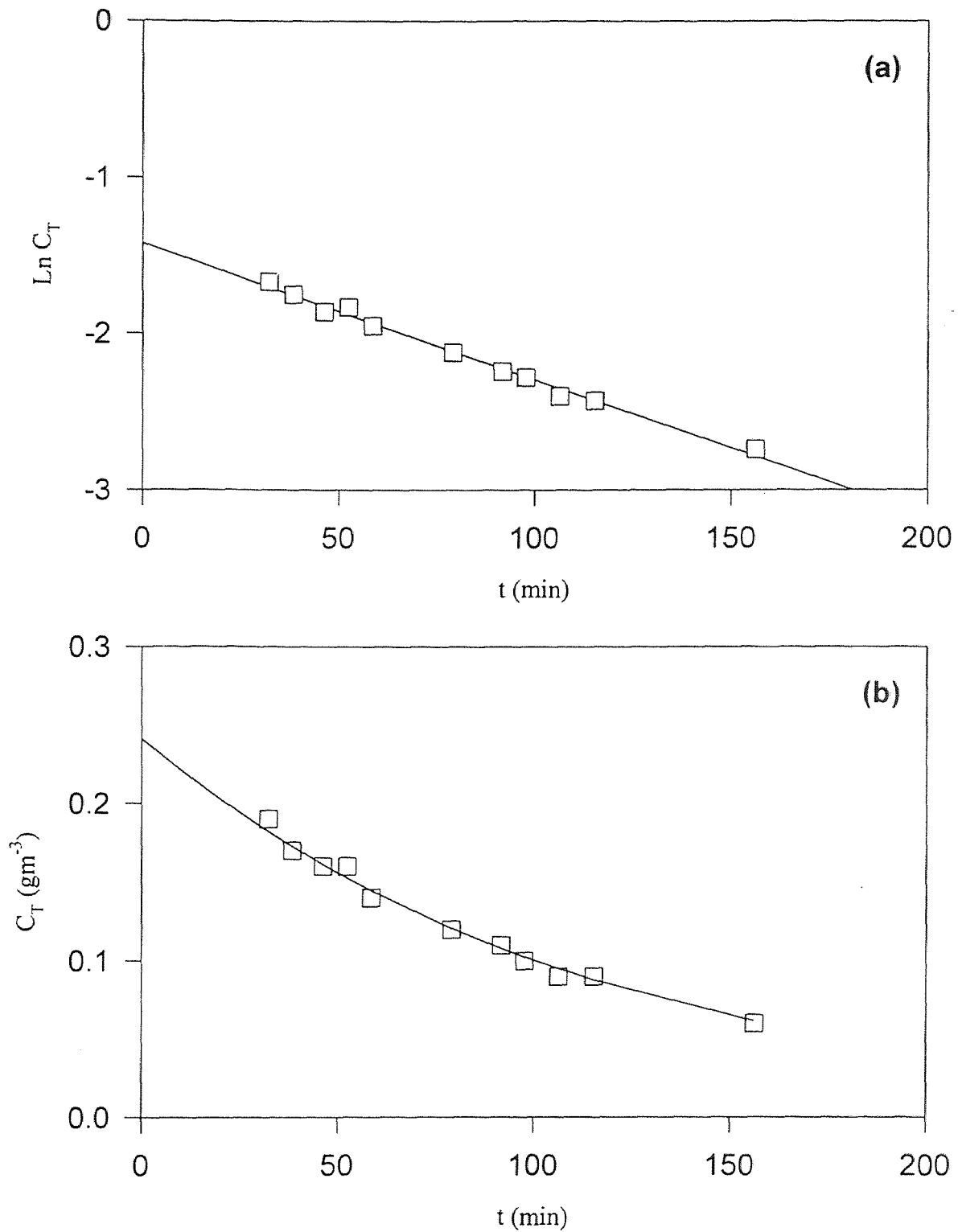


**Figure A-10** Toluene concentration data for experiment E-11 in (a): semilogarithmic and (b): arithmetic scale. Lines and curves represent regressions.

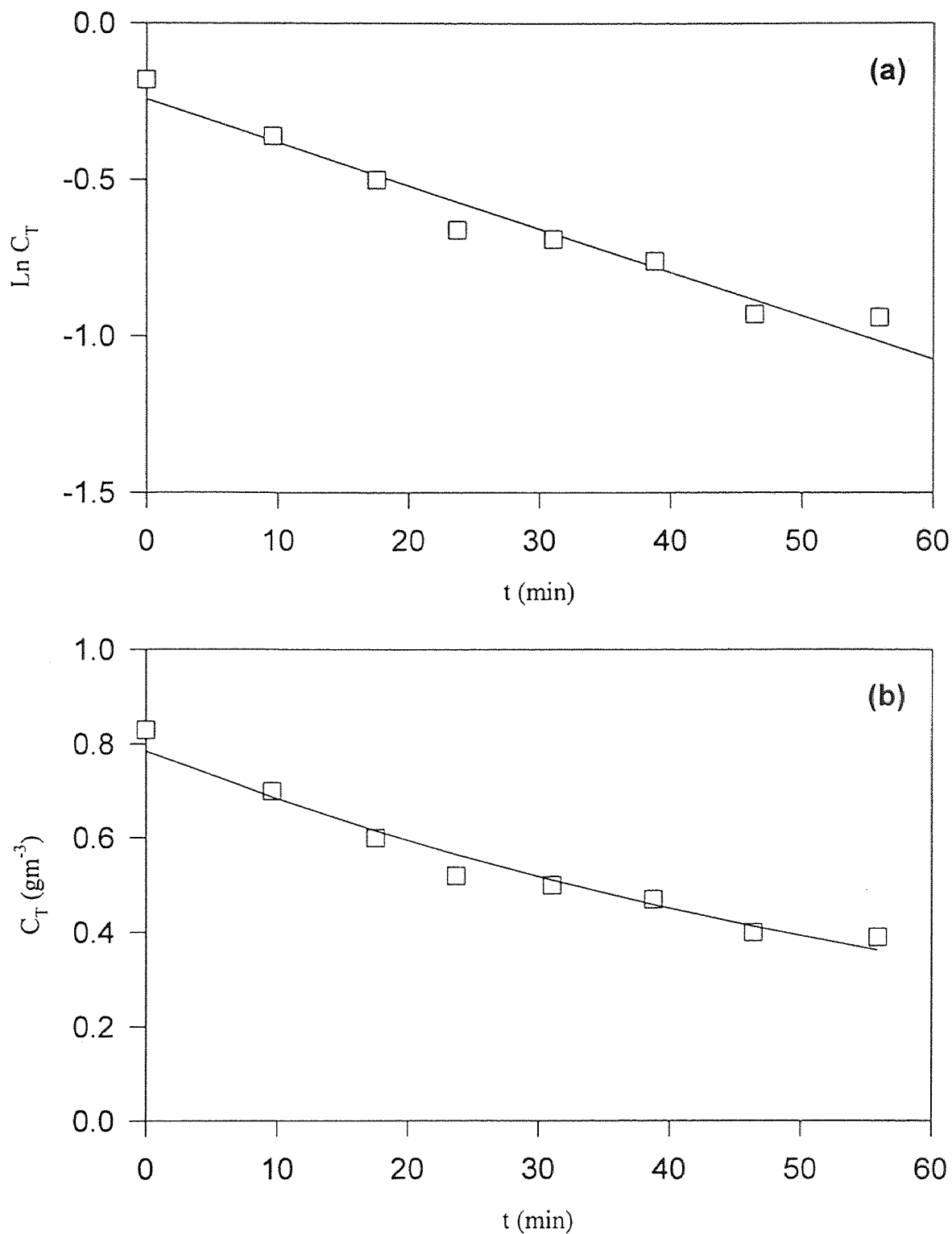


**Figure A-11** Toluene concentration data for the first phase of experiment E-12 (E-12a) in (a): semilogarithmic and (b): arithmetic scale. Lines and curves represent regressions.

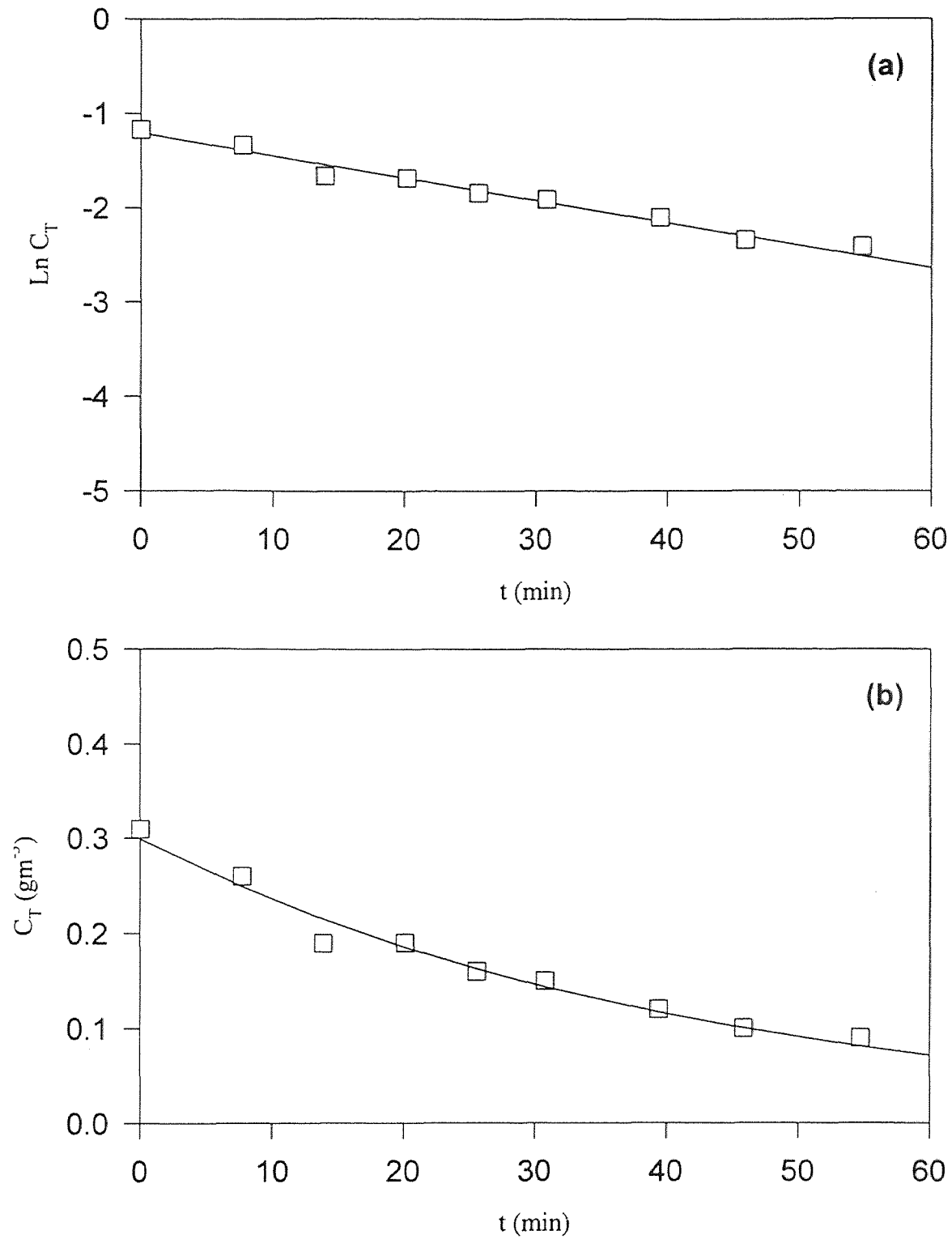


**Figure A-12** Toluene concentration data for the second phase of experiment E-12 (E-12b) in (a): semilogarithmic and (b): arithmetic scale. Lines and curves represent regressions.

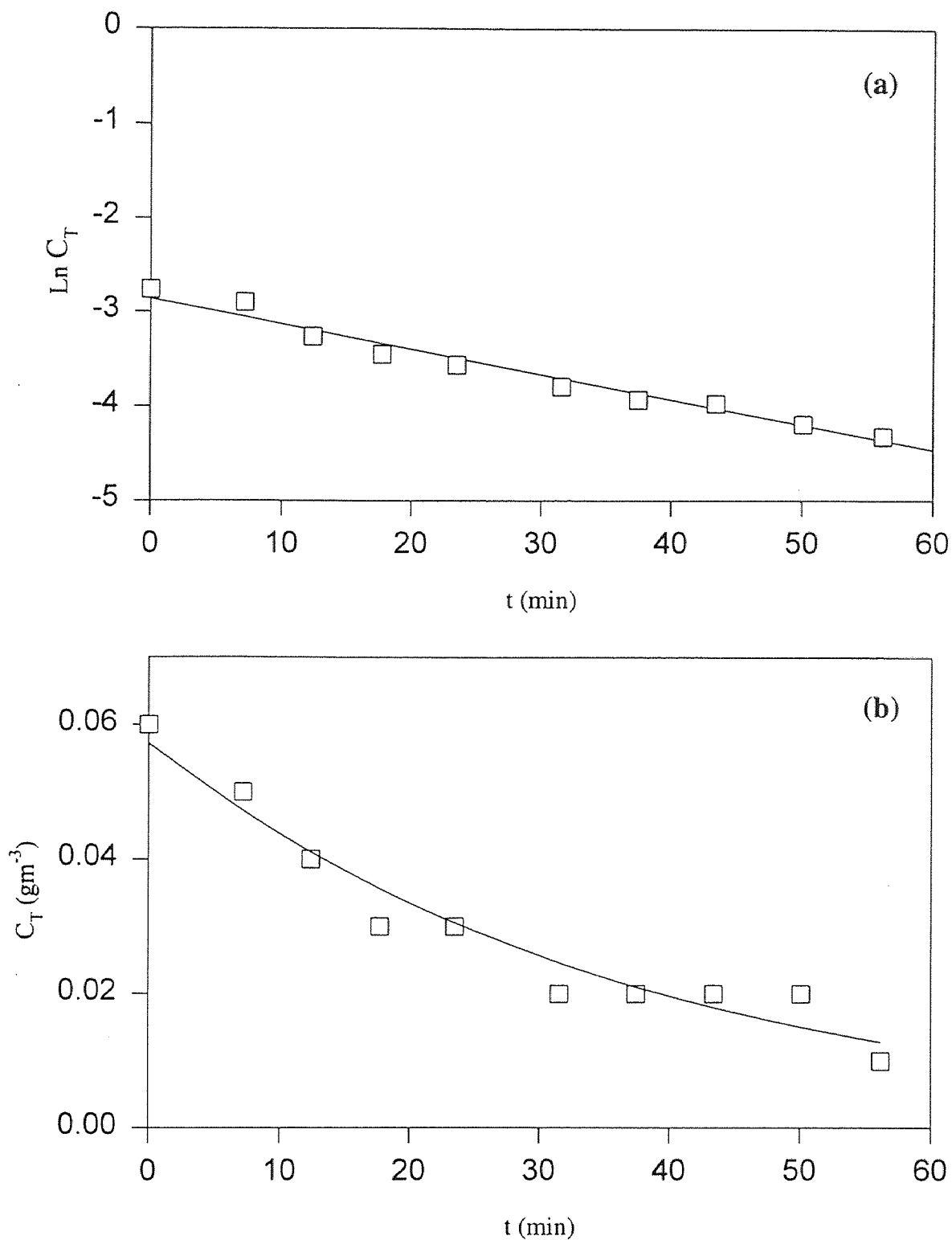


**Figure A-13** Toluene concentration data for the third phase of experiment E-12 (E-12c) in (a): semilogarithmic and (b): arithmetic scale. Lines and curves represent regressions.

**APPENDIX B**

**TOLUENE CONCENTRATION DATA FOR EXPERIMENT B**

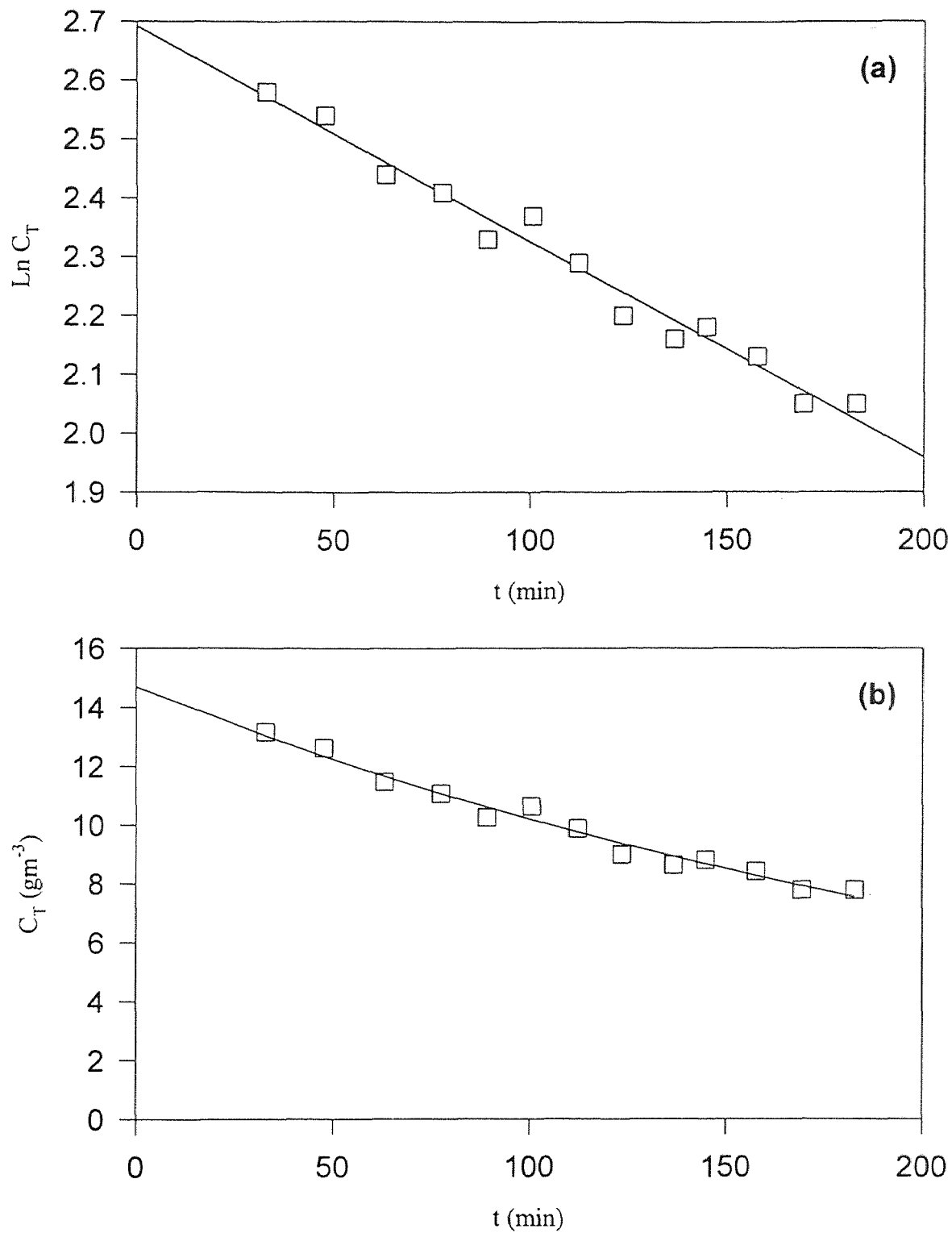


**Figure B-1** Toluene concentration data for the first phase of experiment B (B-1) in (a): semilogarithmic and (b): arithmetic scale. Lines and curves represent regressions.

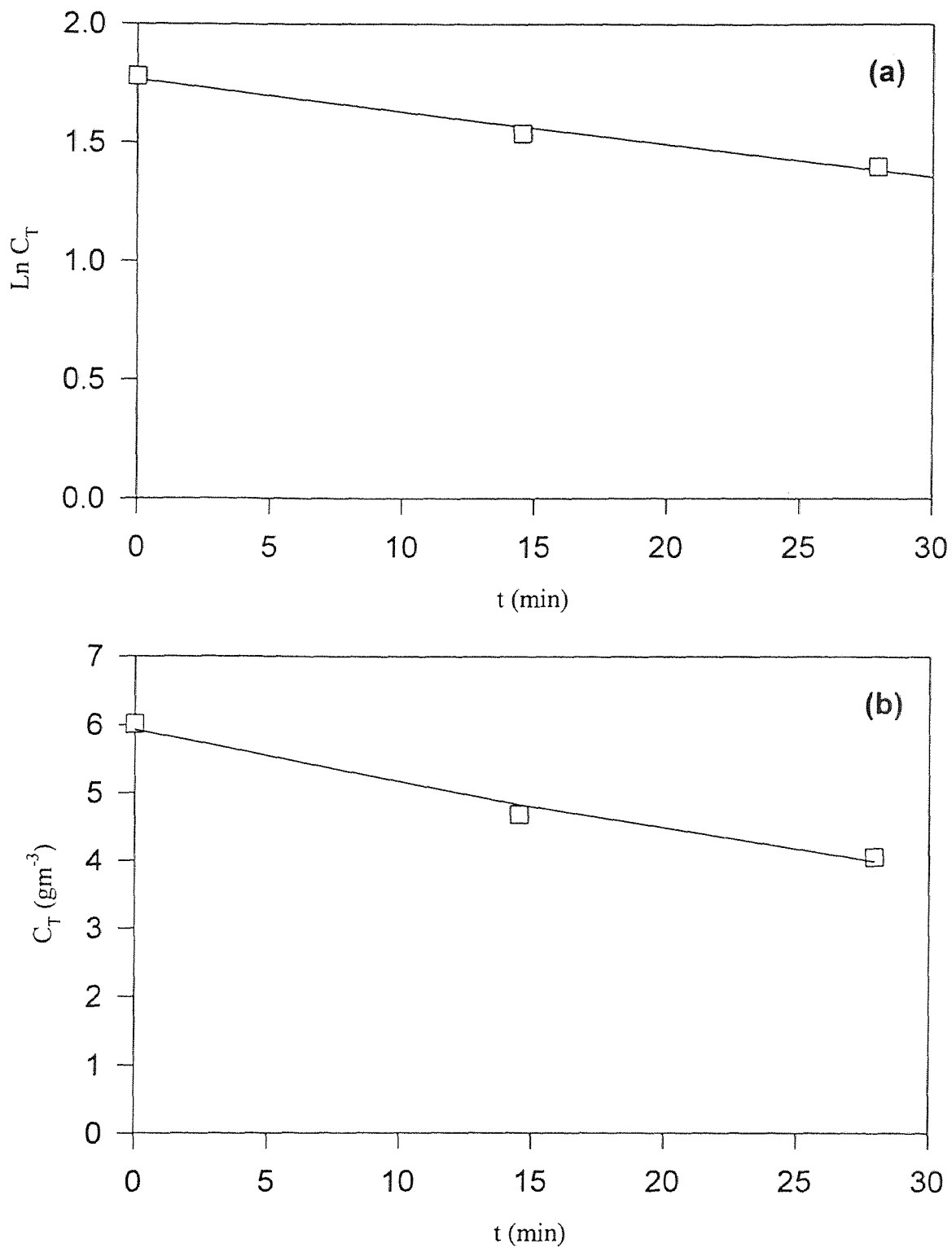


**Figure B-2** Toluene concentration data for the second phase of experiment B (B-2) in (a): semilogarithmic and (b): arithmetic scale. Lines and curves represent regressions.



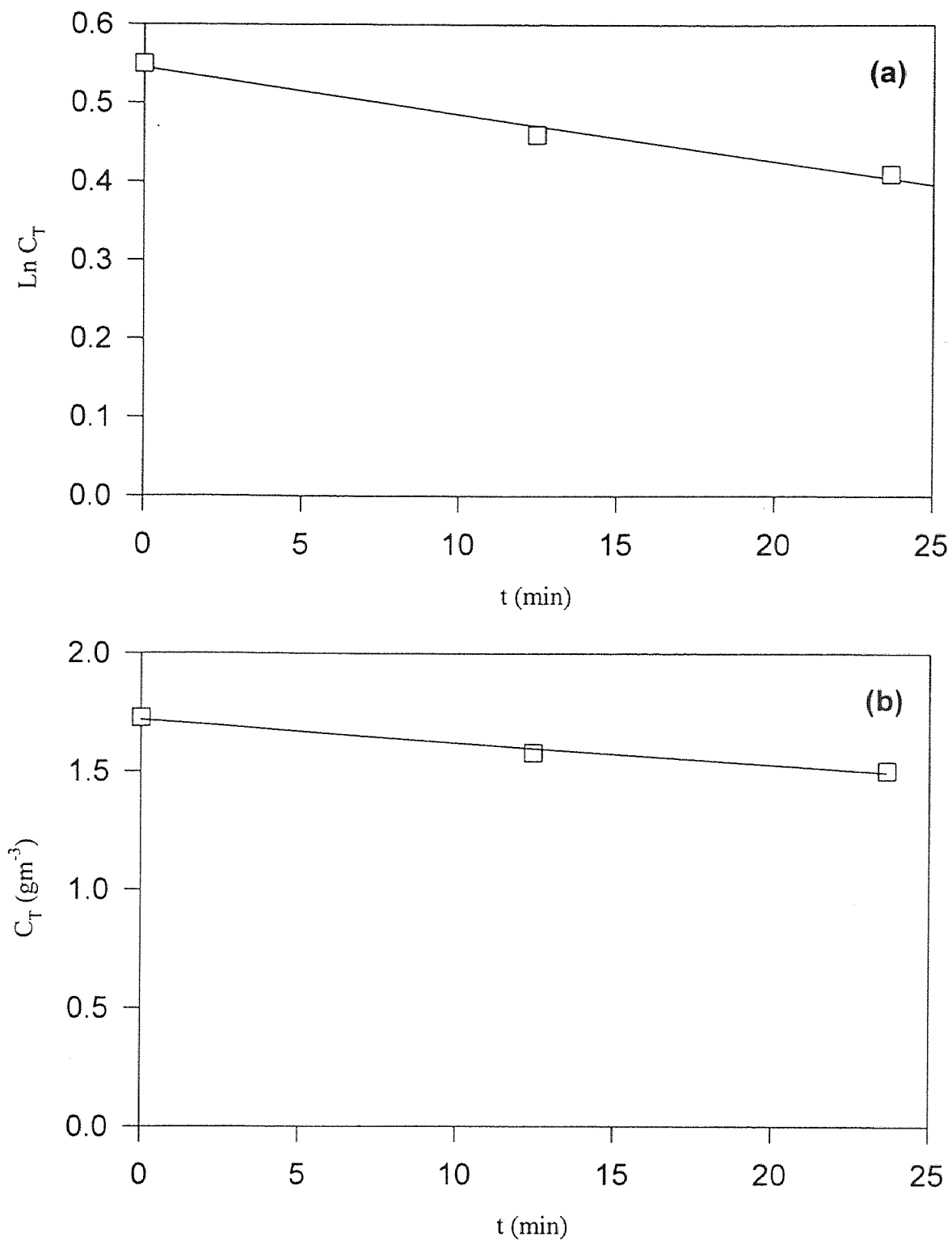


**Figure B-3** Toluene concentration data for the third phase of experiment B (B-3) in (a): semilogarithmic and (b): arithmetic scale. Lines and curves represent regressions.

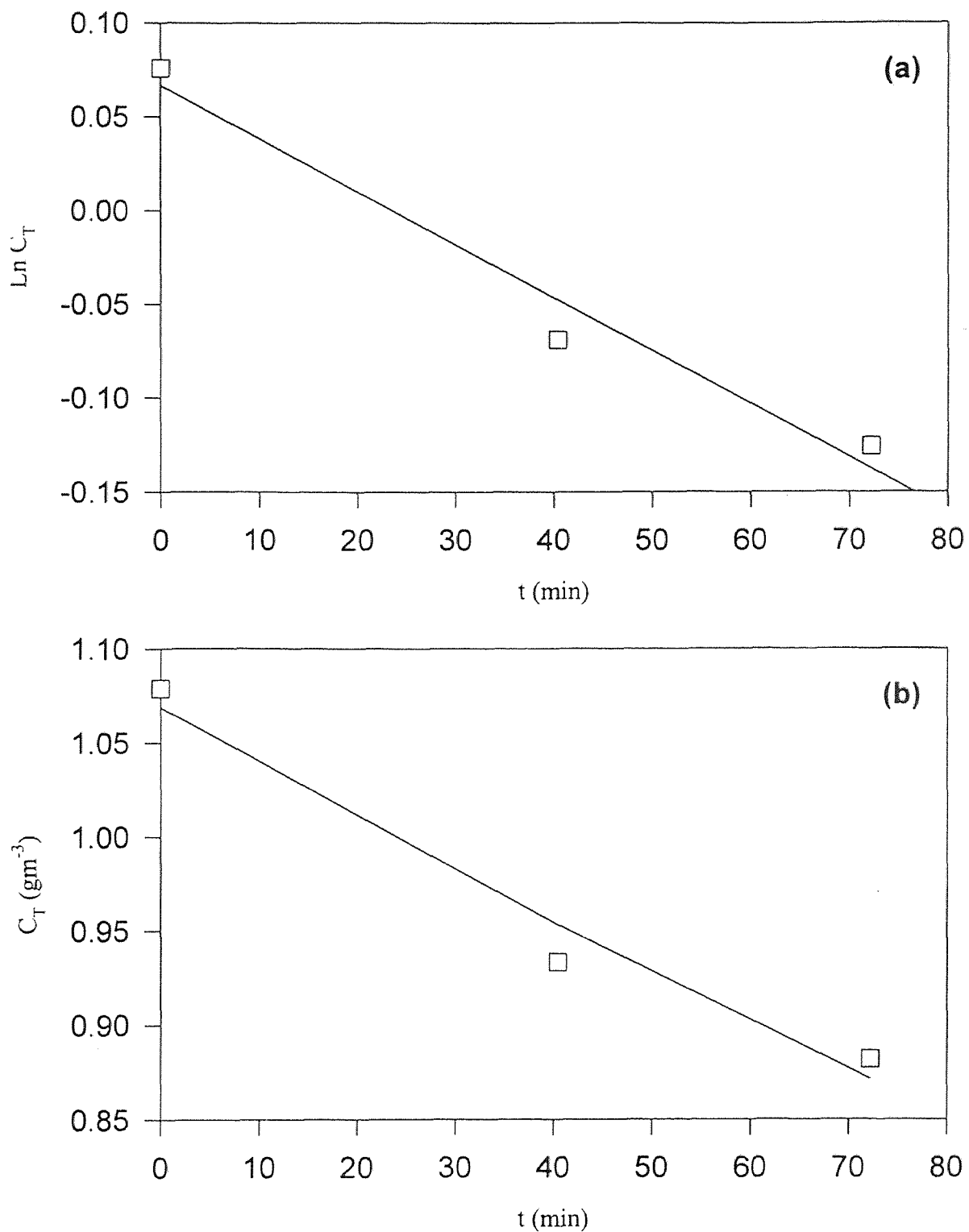


**Figure B-4** Toluene concentration data for the fourth phase of experiment B (B-4) in (a): semilogarithmic and (b): arithmetic scale. Lines and curves represent regressions.

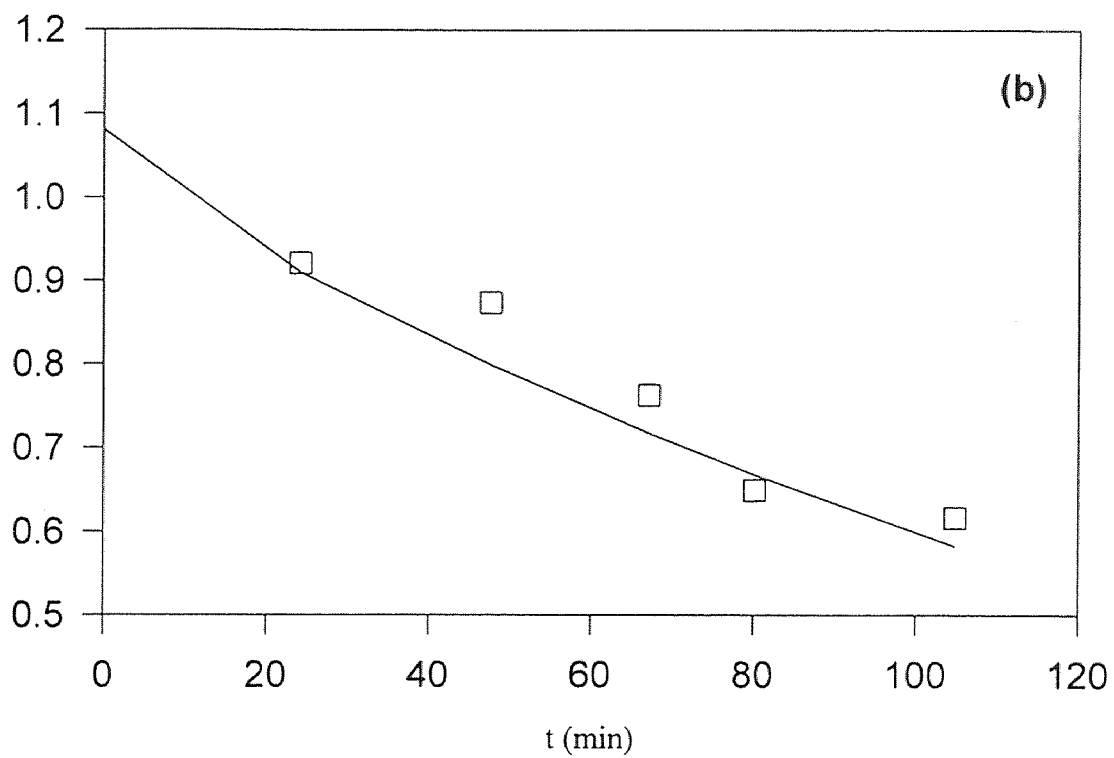
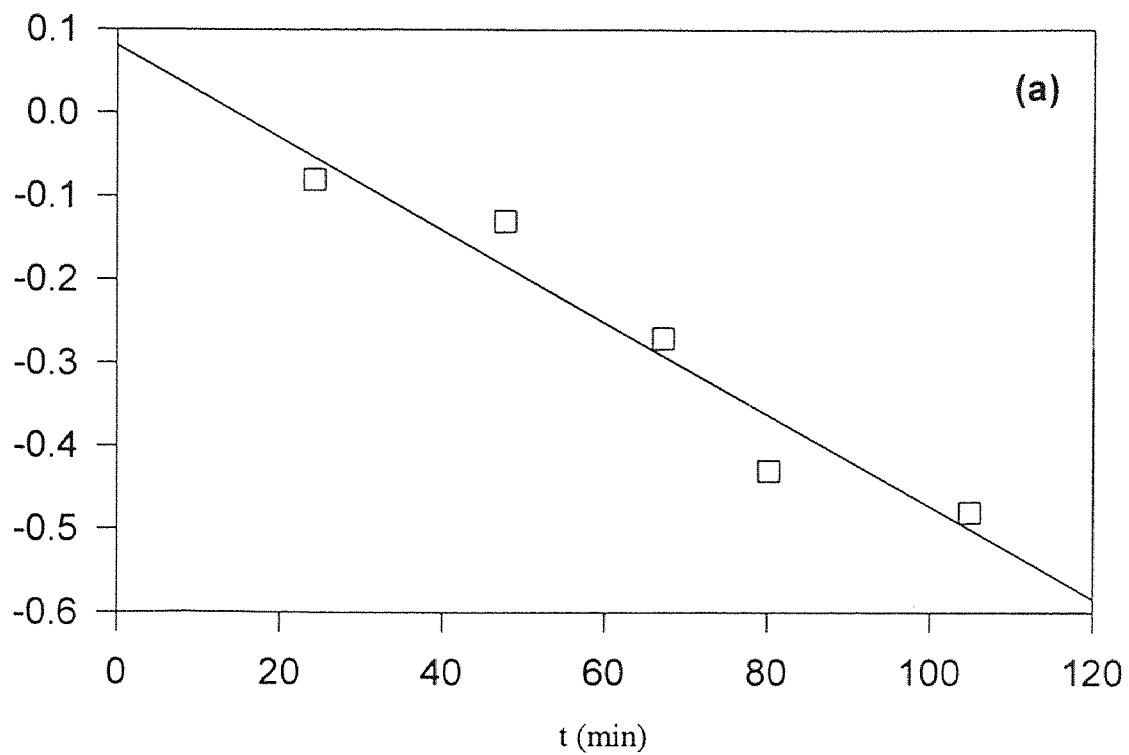


**Figure B-5** Toluene concentration data for the fifth phase of experiment B (B-5) in (a): semilogarithmic and (b): arithmetic scale. Lines and curves represent regressions.

## REFERENCES

1. Androutsopoulou, H. "A Study of the Biofiltration Process Under Shock-Loading Conditions," MS Thesis, Department of Chemical Engineering, Chemistry and Environmental Science, New Jersey Institute of Technology, Newark, NJ, May 1994.
2. Beausoleil, Y.J. and J.S. Huber. "The Use of Air Sparging in the Remediation of a Production Gas Processing Facility," *SPE/EPA Exploration & Production Environmental Conference*, San Antonio, Texas, March 7-10, 1993.
3. Bohn, H., "Biofiltration: Design Principles and Pitfalls," *86th Annual Meeting of Air and Waste Management Association*, Paper No. 93-TP-52A.01, Denver, CO. June 13-18, 1993.
4. Cohen, M.L., "Sensitivity Analysis and Design Calculations with Biofiltration Models," MS Thesis, Department of Civil and Environmental Engineering, New Jersey Institute of Technology, Newark, NJ, January 1996.
5. Deshusses, M.A. and G. Haner, "The Removal of Volatile Ketone Mixtures from Air in Biofilters," *Bioprocess Eng.* 9: 141-146, 1993.
6. Diks, R.M., "The Removal of Dichloromethane From Waste Gases in a Biological Trickling Filter," Ph. D Thesis, Department of Chemical Engineering, The Eindhoven University of Technology, The Netherlands, 1992.
7. Hildebrant, W. and F. Jasiulewicz, "Cleaning Up Military Bases," *The Military Engineer*, 552. September-October:6-9, 1992.
8. Horsby, M. *Site Remediation*, 2nd Edition. CAPCO, Oklahoma, 1995.
9. Kutzer, S. "A Method for Treatment of Waste Water," *Chem. Eng. Technol.* 18: 149-155, 1995.
10. Leson, G., D.S. Hodge, F. Tabatabai, and A.M. Winer. "Biofilter Demonstration Projects for the Control of Ethanol Emissions," *86th Annual Meeting of Air and Waste Management Association*, Paper No. 93-WP-52C.04, Denver, CO, June 13-18, 1993.
11. Leson, G. and B.J. Smith, "Results from the PERF Field Study on Biofilters for Removal of Volatile Petroleum Hydrocarbons," *Proceedings of the 1995 Conference on Biofiltration (an Air Pollution Control Technology)*, D.S. Hodge and F.E. Reynolds, Jr. (eds.), The Reynolds Group, Tustin CA: 99-113, 1995.

12. Li, D.X. "In situ Biofiltration for Treatment of Petroleum Hydrocarbon Vapors," *Proceedings of the 1995 Conference on Biofiltration (an Air Pollution Control Technology)*, D.S. Hodge and F.E. Reynolds, Jr. (eds.), The Reynolds Group, Tustin CA: 1-17, 1995.
13. Naisbitt, J. *Megatrends*, Warner Books, USA 1984
14. Ottengraf, S.P.P. and A.H.C. van den Oever. "Kinetics of Organic Compound Removal from Waste Gases with a Biological Filter," *Biotechnol. Bioeng.*, 25: 3089-3102, 1983.
15. Ottengraf, S.P.P. "Exhaust Gas Purification," pp 425-452, *In: Biotechnology, W. Shnborn (ed.)*, Vol 8, VCH, Verlagsgesellschaft, Weinheim, Germany, 1986.
16. Ottengraf, S.P.P. and R. Disks, "Biological Purification of Waste Gases," *Chimicaoggi*, (1990): 41-45, 1990.
17. Shareefdeen, "Engineering Analysis of a Packed-Bed Biofilter for removal of Volatile Organic Compound (VOC) emissions," Ph. D Thesis, Department of Chemical Engineering, Chemistry and Environmental Science, New Jersey Institute of Technology, Newark, NJ, May 1994.
18. Shareefdeen, Z., B.C. Baltzis, Y.-S. Oh, R. Bartha, "Biofiltration of Methanol Vapors," *Biotechnol. Bioeng.* 41: 512-524, 1993.
19. Stamatiadis, Pothitos, "A methodology for the Design of An Integrated Air Stripping/Biofiltration Process to Clean Contaminated Aquifers," MS Thesis, Department of Civil and Environmental Engineering, New Jersey Institute of Technology, Newark, NJ, January 1997.
20. Zill, M., A. Converti, A. Lodi, M. Del Borghi, and G. Ferraiolo, "Phenol Removal from Waste Gases with a Biological Filter by *Pseudomonas Putida*," *Biotechnol. Bioeng.* 41: 693-699, 1993.